Journal of Materials Science: Materials in Electronics (2019) 30:3222–3243
https://doi.org/10.1007/s10854-019-00701-w

REVIEW

# Recent progress on the development of Sn–Bi based low-temperature Pb-free solders

Fengjiang Wang[1] · Hong Chen[1] · Ying Huang[1] · Luting Liu[1] · Zhijie Zhang[1]

Received: 3 November 2018 / Accepted: 5 January 2019 / Published online: 10 January 2019
© Springer Science+Business Media, LLC, part of Springer Nature 2019

**Abstract**
With the implementation of legislations on inhibiting the usage of Sn–Pb solder in consumer electronic products, Sn–Ag–Cu series solder has been gotten the most application. However, there are some stimulations from electronic manufacturers to adopt low temperature soldering such as the economic driver from the reduction in manufacturing assembly cost and the reliability driver to avoid the dynamic warpage of area array components caused from Sn–Ag–Cu solder. Sn–Bi series solder is one of the promising candidates, which met the requirements for low melting point, low cost and environment friendly. However, the disadvantage of brittleness characteristic prevented its wide practical application. In order to promote the better application of Sn–Bi based solders, many efforts have been made to improve the wettability, mechanical properties and reliability of Sn–Bi based solders. This paper will summarize the related results about Sn–Bi solder alloys from wettability, interfacial reaction, mechanical properties of Sn–Bi solder and reliabilities of Sn–Bi solder joints. Moreover, in order to improve the properties of Sn–Bi solders, researchers have done lots of works on effect of addition of element dopants. The corresponding works of effect of alloying elements on the properties of Sn–Bi solder were also focused. According to the existing research results, it provides an important basis of understanding the current development of Sn–Bi solders.

## 1 Introduction

In electronic industry, Pb-containing Sn–Pb eutectic solder has been used for almost a century due to its good wettability, lower cost, excellent properties and satisfactory reliabilities [1]. However, in the past decade, the development and application of Pb-free solders have been greatly concerned with the implementation of WEEE and RoHS directives [2], and varieties of Pb-free solder alloys have been developed based on Sn-based system. Among them, Sn–Ag–Cu series got the most popular application for their favorable performances [3, 4]. However, a serious problem for Sn–Ag–Cu Pb-free is that its melting point is far higher than Sn–Pb solder (217–221 °C vs. 183 °C), while the electronic assembly industry is currently trying to adopt low temperature soldering based on the following motivations [5, 6]:

- *Technical issue* the trend toward miniaturization on personal electronic devices has driven the need for thinner and smaller area array components. The higher reflow soldering temperature required for Sn–Ag–Cu solder would result in thermal warpage on these components and the board.
- *Reliability issue* under the higher soldering temperature, the solder joint quality was easily deteriorated with the formation of Head-on-Pillow (HoP) due to the warpage of components [7].
- *Economic issue* it is related with energy costs from running the reflow soldering system and material costs from the Ag-contained solders.

To develop the low temperature solder, Zn, In and Bi are the most common used alloying elements for Sn-based solder. Although Sn–9Zn eutectic solder has the lower melting temperature of 198 °C, the weak oxidation resistance and poor wettability from the existence of Zn have strictly restricted its massive application [8, 9]. Sn–In has the melting temperature of 118 °C at the eutectic composition of Sn–52In, and is an ideal low temperature solder with good ductility, fatigue life and wettability [10]. However, due to the high cost from indium, it is locally

✉ Fengjiang Wang
fjwang@just.edu.cn

[1] Provincial Key Laboratory of Advanced Welding Technology, Jiangsu University of Science and Technology, Zhenjiang 212003, China

used in some advanced and specialized packaging [11]. In recent years, Sn–Bi solder has gotten much attention due to its lower melting point. The melting point of 138 °C at Sn–58Bi eutectic is lower than that of Sn–Pb solder. Additionally, the cost of Bi is cheaper. Therefore, Sn–Bi solder is a promising alloy and an ideal choice for the mass application of low temperature soldering in electronic industry [12, 13]. However, there still exists some disadvantages such as poor wettability and the brittleness of alloys induced from the inherent brittleness of Bi element. Additionally, Bi is easy to be coarsened at high temperature, which led to the deterioration on the plasticity and ductility [14, 15].

In order to improve the properties of Sn–Bi solder, many researchers have tried to incorporate the additional alloying elements. Therefore, this paper mainly reviewed the current development of Sn–Bi based solder from the following several aspects: wettability, microstructure, intermetallic compound (IMC) layers at the interface of solder joints, mechanical properties of solder or joints and the reliability of solder joints.

## 2 Wettability

Wettability is one of the important indicators to measure the solderability of solders. Usually, it can be evaluated by the contact angle ($\theta_C$) from spreading test shown in Fig. 1. With the molten solder spreading over the substrate, the wettability depends on the ability of the molten solder to react with the substrate, and is decided by the formation of interfacial IMCs and the surface tensions between solid–liquid ($\gamma_{SL}$), liquid–flux ($\gamma_{LF}$) and solid–flux ($\gamma_{SF}$). The contact angle $\theta_C$ is then calculated from these surface tensions by following Young's equation:

$$\cos\theta_c = \frac{\gamma_{SF} - \gamma_{SL}}{\gamma_{LF}}. \quad (1)$$

The wettability of Sn–58Bi solder was firstly studied and compared with Sn–37Pb solder by Mei and Morris [13]. The calculated wetting angle on Cu substrate for Sn–58Bi solder and Sn–37Pb solder was ~35° and 25°, respectively. In common sense, the smaller the wetting angle $\theta_C$ is, the better the wettability of solder alloys is. Therefore, Sn–58Bi solder had a poorer wettability than Sn–37Pb solder.

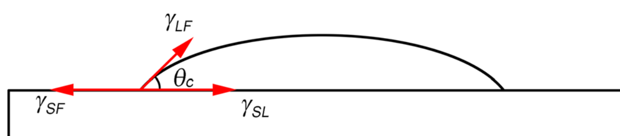


**Fig. 1** Spreading of solder alloy on the substrate

To improve the wettability of Sn–Bi solder, the effect of different content of In addition was studied by Chen et al. [16]. With In addition, the wettability of solders increased until In content was reached to 4 wt%, and then decreased with further addition of In due to the formation of Cu–Sn–In IMCs at the interface. Dong et al. [17] studied the effect of trace amounts of rare earth (RE) and Ag addition on the wettability of Sn–58Bi solder, and found that RE had better effect on improving the wettability of solder than Ag element. Furthermore, Sn–Bi solder had the best wettability with the addition of both Ag and RE. The addition of Ni nanoparticles on the contact angle of Sn–Bi solder alloy was investigated by Gain and Zhang [18]. The results indicated nano Ni addition decreased the contact angle of solder on Cu substrate because Ni nano particles were reacted with Sn to produce $NiSn_4$, which was finely distributed in the solder matrix and promoted the wettability. Yang et al. [19] also investigated the effect of Mo nanoparticles on wettability of Sn–58Bi solder, and found 0.25 wt% Mo was helpful to increase the wettability of solder. Liu et al. [20] added nano Cu into Sn–58Bi solder paste, but the results indicated that the wettability of solder on Cu substrate was deteriorated with the addition of nano Cu.

Some chemical compounds were also added into Sn–Bi solder to improve the solder wettability. Yang et al. [21] found that the addition of 1 wt% $BaTiO_3$ into Sn–58Bi solder could improve the wettability by about 10% compared with Sn–58Bi solder. Liu et al. [22] observed that about 1 wt% addition of $Y_2O_3$ into Sn–58Bi solder improved the wettability of solder. Yang et al. [23] reported the effect of nano sized graphite addition on wettability of Sn–58Bi solder, but the results indicated that the wettability of Sn–Bi solder decreased with the addition of nano sized graphite. Oh and Lee [24] tried to dope small amounts of Pd, Co, Zn or Ni-organic compounds into Sn–57.6Bi–0.4Ag solder. The results showed that the addition of Pd-organic compounds decreased the wetting angle of solder alloy, while the addition of Co, Zn or Ni-organic compounds increased the wetting angle. It is believed that the Pd-doped Sn–57.6Bi–0.4Ag alloy had the superior wettability due to the antioxidant nature of Pd.

Besides the addition of alloying elements, the content of Bi and wetting temperature also played effects on the wettability of Sn–Bi solder. Lee et al. [25] studied the wettability of Sn–Bi solder with Bi content from 5 to 58 wt%, and found that the wettability decreased with Bi content, but improved with the wetting temperature. Chen et al. [26] carried out the spreading ratio ($S_R$) test for Sn–xBi–3Zn and Sn–38Bi–xZn

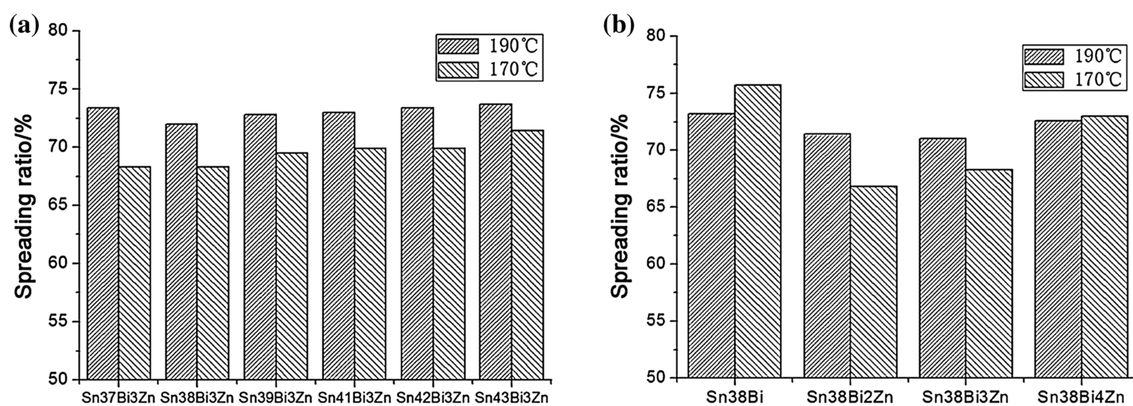


**Fig. 2** The spreading ratios of **a** Sn–xBi–3Zn and **b** Sn–38Bi–xZn solders at 170 °C and 190 °C [26]

solders at 170 °C and 190 °C, and the results were shown in Fig. 2. The spreading ratio is defined as

$$S_R = \frac{D - H}{D} \times 100\%, \quad (2)$$

where $H$ stands for the height of solders after spreading and $D$ is the diameter of solder balls used for spreading test. The higher the spreading ratio is, the better the wettability of solder is. The change of Bi content had no significant effect on the wettability. However, increasing the wetting temperature could improve the wettability of solders because the activity of molten solder was enhanced and the interaction between the molten solder and the substrate became more intensive. The authors also found that Zn addition would deteriorate the wettability. Zhang et al. [27] studied the effect of Bi content in Sn–xBi–1.8Sb solders and Sb content in Sn–48Bi–xSb solders on wettability of solders, as shown in Fig. 3. The highest spreading ratio was reached at Bi content of 48%. With the addition of Sb element, the wettability firstly increased with Sb addition and then dropped. Also, the organic flux played the better effect on the wettability of Sn–Bi solders compared with resin flux due to its capability of removing the oxidation film.

Table 1 summarized the effective alloying elements that can be used to improve the wettability of Sn–Bi solders. As seen from Eq. (1), the addition of alloying elements would alter the surface tension of molten solder ($\gamma_{SL}$), and played the positive role on the wettability.

## 3 Microstructure of Sn–Bi based solders

The microstructure of solder alloys will obviously affect the mechanical properties of solder or solder joints. For the sake of improving the microstructure of Sn–Bi based solders, the Bi content in Sn–Bi solder was altered and some other alloying elements were added into Sn–Bi solders.

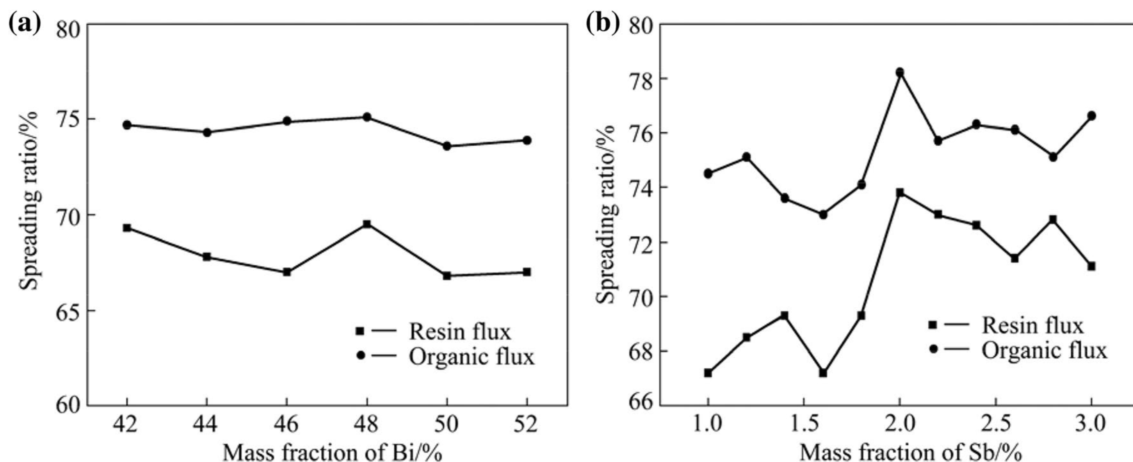


**Fig. 3** Spreading ratios of **a** Sn–xBi–1.8Sb alloys and **b** Sn–48Bi–xSb alloys at 190 °C [27]

**Table 1** Improvement on wettability of Sn–Bi based solders by alloying elements

| Sn–Bi based solders | Wettability |
|---|---|
| Sn–Bi–Ag [28] | The increase on Ag content was helpful to decrease the wetting angle under $N_2$ + 10% $H_2$ atmosphere |
| Sn–Bi–$BaTiO_3$ [21] | Sn–58Bi–1% $BaTiO_3$ had larger spreading coefficient than Sn–58Bi solder |
| Sn–Bi–Cu [29] | Cu addition caused the concentration of Cu at the interface which favored for reducing the wetting angle of solders |
| Sn–Bi–In [16] | The addition of In with content lower than 4 wt% was helpful to increase the wettability of Sn–Bi solder |
| Sn–Bi–nano Mo [19] | 0.25 wt% Mo nanoparticles was helpful to increase the wettability |
| Sn–Bi–nano Ni [18, 30] | Sn–58Bi–Ni had lower contact angle than Sn–58Bi solder |
| Sn–Bi–RE [17] | The addition of RE element to Sn–58Bi solders had better wettability |
| Sn–Bi–Sb [27] | The addition of Sb with content lower than 2 wt% increased the wettability of Sn–48Bi solder |
| Sn–Bi–$Y_2O_3$ [22] | The addition of $Y_2O_3$ improved the wettability of Sn-58Bi solder, and the optimum content of $Y_2O_3$ was 1 wt% |

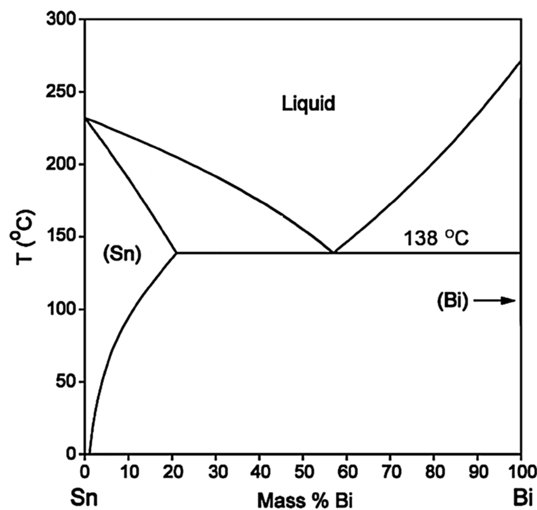


**Fig. 4** Sn–Bi phase diagram

From Sn–Bi phase diagram shown in Fig. 4, the eutectic reaction is occurred at 138 °C between Sn and Bi at the composition of Sn–58Bi. The microstructure of Sn–Bi solder is composed of β-Sn and Bi phases. Moreover, Bi atoms can be dissolved into β-Sn phases to form the solid solution with the maximum solubility of 20.5 wt% [31].

To investigate the effect of Bi content on the microstructure of Sn–Bi solder, Wang et al. [32] and Lai and Ye [33] investigated the microstructures of Sn–Bi solders with the compositions of solid solution, hypo-eutectic and eutectic. Figure 5 shows the microstructural evolution of Sn–Bi solder with different Bi content. The microstructures of Sn–5Bi and Sn–15Bi solid solution solders were constituted by Bi particle and β-Sn phase. The microstructure of Sn–30Bi hypo-eutectic solder was consisted of eutectic phase and primary β-Sn phase. The microstructure of Sn–58Bi eutectic solder was composed of lamellar β-Sn phase and Bi phase.

To improve the mechanical properties of Sn–Bi based solder, many researchers have done lots of works on incorporating the alloying elements into Sn–Bi solder. Accordingly, the alloying elements will also change the microstructure of solder alloys. Mokhtari and Nishikawa [34] studied the microstructure of eutectic Sn–Bi, (Sn–Bi)–0.5In, and (Sn–Bi)–0.5Ni solders. As shown in Fig. 6, 0.5 wt% addition of In did not enroll in the reaction to change the microstructure of Sn–58Bi eutectic solder, but Ni addition was reacted with Sn to produce Ni–Sn IMC ($Ni_3Sn_4$) in the structure. Further, Chen et al. [16] tried to incorporate more In with the content of 1–5 wt% into Sn–Bi solder, as shown in Fig. 7. With 1–3 wt% In addition, more β-Sn dendrites were produced in the structure, while with 4–5 wt% In addition, besides the formation of large amounts of β-Sn dendrites, Bi–In IMCs were also observed in the eutectic structure. Li et al. [35] also observed the microstructure of Sn–Bi–In solders with the content of In at 12 wt% but the content of Bi changing from 35 to 50 wt%, and got the similar microstructure containing β-Sn, Bi, and InBi phases. Decreasing on Bi content led to less Bi phases in the structure.

The effect of Sb addition on Sn–Bi-based solders was investigated by Zhang et al. [27].The results showed that Sn–48Bi–xSb solders were consisted of Sn phase, Bi phase and Sn–Sb intermediate phase. With the increasing on Sb addition, Sn–Sb intermediate phases increased. Chuang and Wu [36] found that the addition of 0.5 wt% RE Ce could obviously refine the microstructure of Sn–58Bi solder due to the increase on the number of heterogeneous nucleation sites for solidification provided by $Ce(Bi, Sn)_3$ intermetallic phases. Shen et al. [37] studied the effect of 0.25 or 0.5 wt% RE addition on the microstructures of Sn–30Bi–0.5Cu and Sn–35Bi–1Ag solders, and found trace amounts of RE addition similarly refined the microstructure of β-Sn phase, $Cu_6Sn_5$ and $Ag_3Sn$ IMCs in solders.

Shen et al. [38] investigated the effects of Cu and Zn addition on the microstructure of Sn–40Bi based solder. Due to the addition of Cu and Zn, Bi-rich phases were refined with the morphology of Bi phases transforming from rod-like lamellar into fine globular structures. Cu was existed as $Cu_6Sn_5$ phases, which were entrapped into Bi-rich phase. Zn was existed as the uniform globular $Cu_5Zn_8$ particles

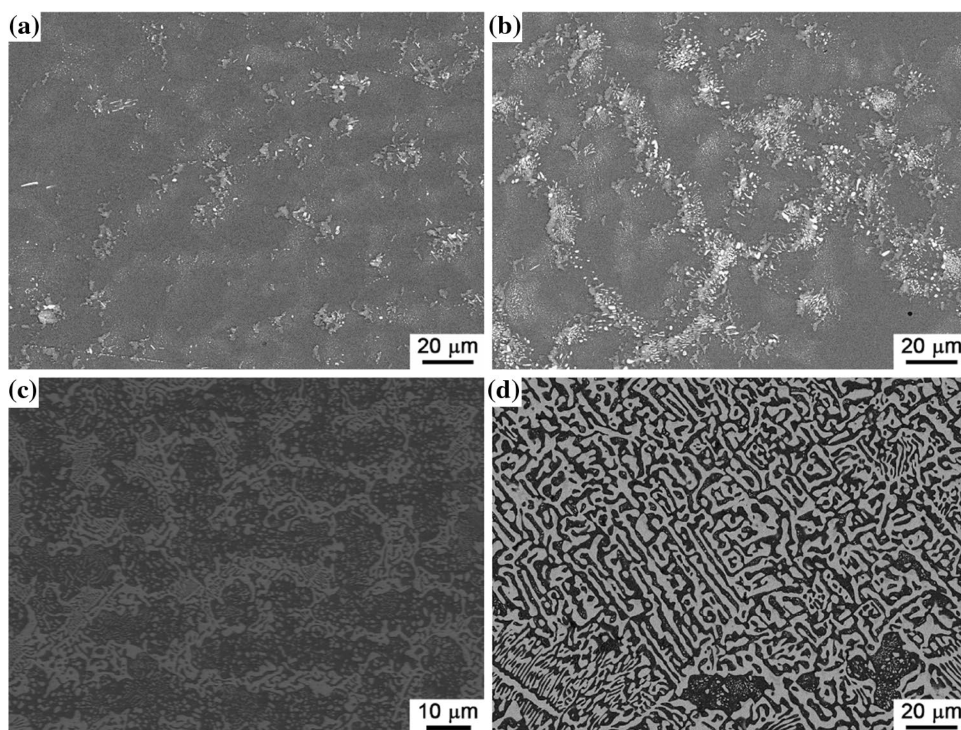


**Fig. 5** Microstructure of Sn–xBi solder alloy: **a** Sn–5Bi, **b** Sn–15Bi, **c** Sn–30Bi, and **d** Sn–58Bi [32]

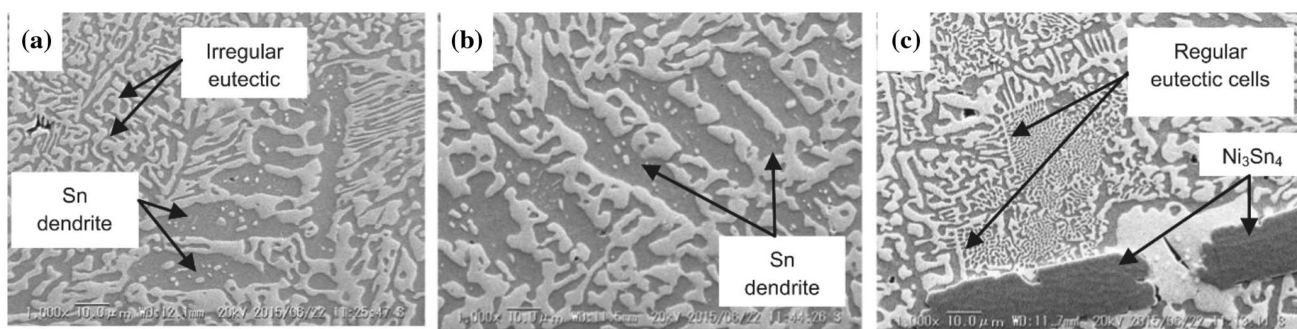


**Fig. 6** Microstructure of Sn–Bi solders: **a** eutectic Sn–Bi, **b** (Sn–Bi)–0.5In, and **c** (Sn–Bi)–0.5Ni [34]

and needle-like Zn-rich phases. Chen et al. [26] studied the microstructure of Sn–38Bi based solder with 2–4 wt% Zn addition. With addition of Zn, the size and proportion of needle-like Zn-rich phase increased in the microstructure. Wang et al. [39] incorporated 0.005 wt% Al or 0.005 wt% P on the basis of Sn–40Bi–2Zn, and found that Al/P addition furtherly refined the microstructure of Bi phases due to the increase on nucleations sites from the formation of $Al_6Zn_3Sn$ and $SnP_3$ phases.

Therefore, one of the obvious advantages from alloying elements into Sn–Bi solder was to refine the microstructure. Refined microstructure is helpful to improve the mechanical properties of solder, which will be summarized later. Li et al. [40] studied the effect of W addition on the microstructure of Sn–57.6Bi–0.4Ag solder. The microstructure was obviously refined due to the W addition. Dong et al. [17] investigated the effect of RE, Ag addition on the microstructure of Sn–58Bi solder. It was suggested that the RE/Ag element addition into Sn–58Bi was helpful to refine the microstructure of solder. Other chemical compounds such as $BaTiO_3$ particles [21], $Y_2O_3$ particles [22] were also verified to be effective on refining the microstructure of Sn–Bi solder. In recent years, the nano materials were also introduced into Sn–Bi solder to improve the microstructure and properties of solder. Ma and Wu [41] studied the effect of different addition of graphene nano sheets (GNSs) into Sn–58Bi–0.7Zn solder. As seen from the microstructure shown in Fig. 8, with increasing of GNSs, the microstructure of Sn–Bi and its composite solder was gradually refined because GNSs

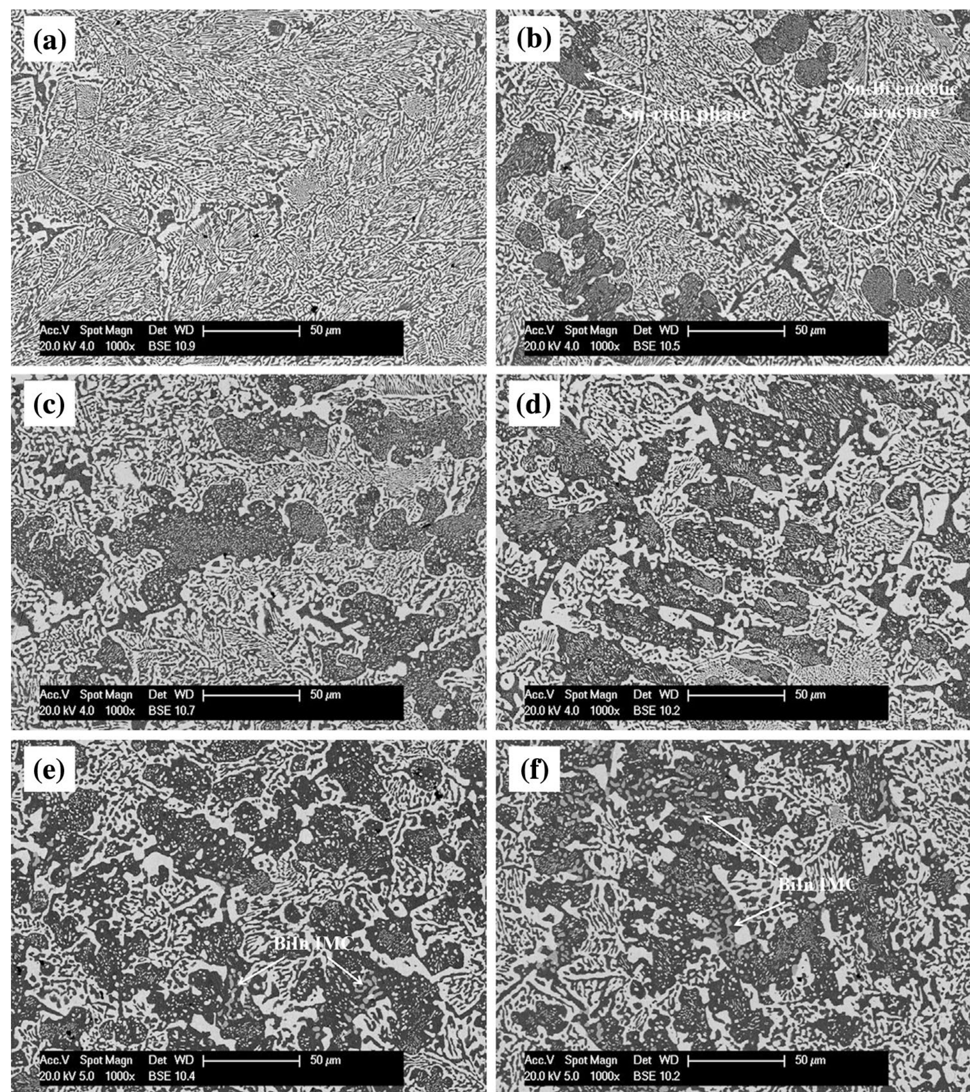


**Fig. 7** Effect of In addition on the microstructure of Sn–Bi based solders: **a** 42Sn–Bi, **b** 42Sn–Bi–1In, **c** 42Sn–Bi–2In, **d** 42Sn–Bi–3In, **e** 42Sn–Bi–4In and **f** 42Sn–Bi–5In [16]

provided more nucleation sites. The refined effect from GNSs on Sn–58Bi solder was also observed by Yang et al. [23, 42]. He et al. [43] investigated the addition of carbon nanotubes (CNTs) to Sn–58Bi solder, and indicated that the CNTs addition led to significant decreasing on the number of dendrites and the refined microstructure. Zhou et al. [44] found that 0.5 or 1 wt% Zn into Sn–58Bi solder was also helpful to refine the microstructure.

As discussed above, it was concluded that different Bi content solders had different phase composition. With adding other elements into the solder new phases were formed and the microstructure was refined. Table 2 lists the change on the microstructures of Sn–Bi based systems from different alloying elements. To sum up, minor addition of alloying elements into Sn–Bi based solders is an effective method to obtain the better microstructure.

## 4 Interfacial structure in Sn–Bi based solder joints

The IMC layer will be formed at the interface when the molten solder wets on the substrate. A thin layer of IMC during soldering ensures the metallic bonding between solder and substrate, and will improve the strength of solder joints. However, the growth of IMC layer is usually occurred during the following service or aging condition, which will degrade the strength and reliability of solder joints due to the brittle and hard nature a of IMCs [46]. Therefore, the researchers have done a lot of studies about the interfacial IMCs in Sn–Bi solder joints, such as the effect of Bi addition, IMC growth during aging condition and the effect of alloying elements.

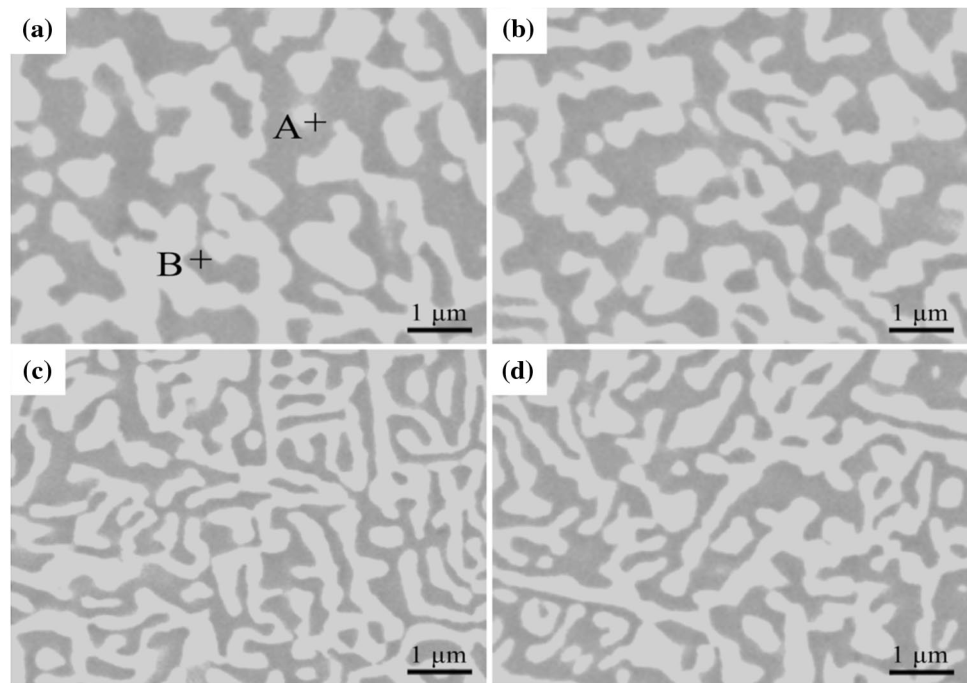


**Fig. 8** Effect of different content of GNSs addition on the microstructure of Sn–Bi solder: **a** Sn–58Bi–0.7Zn, **b** Sn–Bi–Zn–0.038GNS, **c** Sn–Bi–Zn–0.076GNS and **d** Sn–Bi–Zn–0.114GNS solder [41]

**Table 2** Microstructures of Sn–Bi based solders bearing alloying elements

| Sn–Bi based solders | Microstructure |
|---|---|
| Sn–Bi–Ag [17] | Ag addition into Sn–Bi solder produced new $Ag_3Sn$ IMCs in the solder matrix and refined the microstructure |
| Sn–Bi–Ag–W [40] | W addition furtherly refined the microstructure of Sn–Bi–Ag solder |
| Sn–Bi–$BaTiO_3$ [21] | The addition of $BaTiO_3$ refined the microstructure of Sn–58Bi composite solder |
| Sn–Bi–Ce [36] | Ce addition produced Bi–Ce–Sn IMCs in the solder matrix and refined the microstructure of Sn–58Bi solder |
| Sn–Bi–CNTs [43] | CNTs addition significantly decreased the number of dendrites of composite and refined the microstructure of the composite |
| Sn–Bi–Cu [29] | The addition of Cu produced $Cu_6Sn_5$ IMCs in the solder matrix |
| Sn–Bi–Fe [45] | Fe addition produced FeSn, $FeSn_2$ phases |
| Sn–Bi–GNSs [23, 42] | GNSs addition refined the microstructure of Sn–Bi composite solder |
| Sn–Bi–In [16, 35] | In addition into Sn–Bi solder produced Bi–In IMCs in the solder matrix |
| Sn–Bi–Ni [34] | Ni addition into Sn–Bi solder produced new $Ni_3Sn_4$ IMCs |
| Sn–Bi–Sb [27] | Sb addition into Sn–48Bi solder produced SnSb intermediate phases |
| Sn–Bi–$Y_2O_3$ [22] | $Y_2O_3$ addition depresses the coarsening rate of phases in Sn–Bi solder matrix during aging |
| Sn–Bi–Zn [26] | In Sn–38Bi solder matrix, 2–5 wt% Zn addition produced needle-like Zn-rich phase |
| Sn–Bi–Zn [44] | In Sn–58Bi solder matrix, 0.5 or 1.0 wt% Zn addition refined the microstructure of Sn–Bi solder |
| Sn–Bi–Zn–Cu [38] | Further addition of Cu into Sn–Bi–Zn solder refined Bi-rich phase |
| Sn–Bi–Zn–Al/P [39] | Further addition of Al or P refined the microstructure |
| Sn–Bi–Zn–GNSs [41] | The GNSs doping could suppress the growth and coarsening of solder microstructure |

In case of the effect of Bi content in Sn–Bi solders on IMC growth, Kang et al. [47] compared the growth kinetics between pure Sn/Cu and Sn–10Bi/Cu solder joints. It was suggested that due to Bi addition, the interfacial reaction between Sn and Cu was enhanced, and the IMC in Sn–10Bi joint developed more quickly than that in pure Sn/Cu joint. Wang et al. [32, 48] systematically studied the effect of Bi content from 2.5 to 58 wt% in Sn–Bi solders on the IMC growth during isothermal aging, and the results were shown in Fig. 9. The interfacial IMCs for Sn–Bi solders on Cu substrate were composed of $Cu_6Sn_5$ and $Cu_3Sn$ according to Sn–Bi–Cu ternary system [49], which was similar as most of Sn-based Pb-free solders. With Bi content increasing in Sn–Bi solder, the growth rate of interfacial IMC obviously

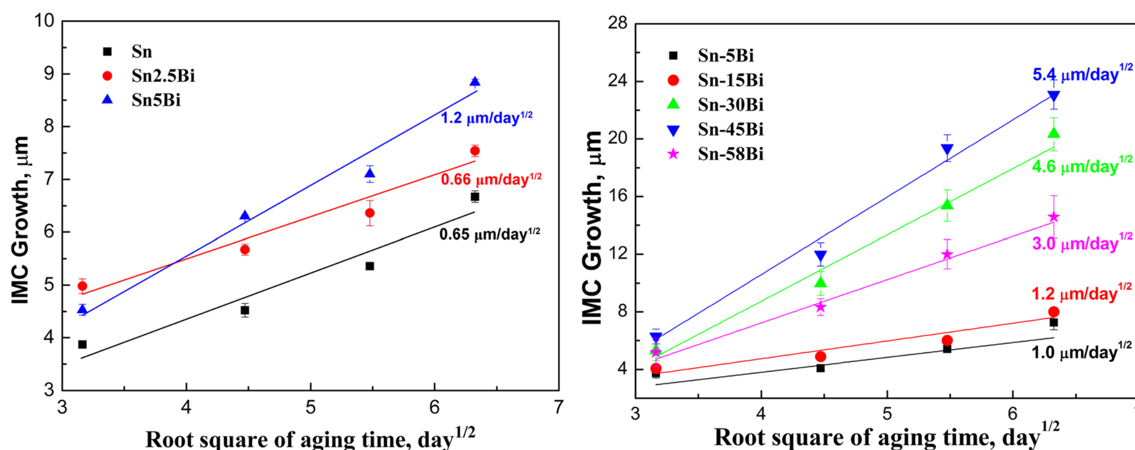


**Fig. 9** IMC growth in Sn–Bi joints with the effect of Bi content during isothermal aging [32, 48]

increased. It should be noted that Sn–58Bi solder had a lower growth rate than Sn–45Bi solder because the authors suggested that the formation of continuous Bi-rich layer between solder and IMC inhibited the atomic diffusion in Sn–58Bi solder. It seems Bi addition will accelerate the IMC growth at the interface. Firstly, the melting point ($T_m$) of solder decreases with Bi addition, and accordingly the higher homologous temperature $T/T_m$ will accelerate the atomic diffusion. Secondly, Bi existence in the solder will inhibit the diffusion of Cu atoms from substrate into the solder matrix and mostly be accumulated at the interface to produce IMCs.

However, besides the over growth on IMC layer, there still exists some problems with the formation and growth of interfacial IMC in Sn–Bi solder joints. Hu et al. [50] studied the interfacial reaction between molten Sn–58Bi solder and Cu at different temperature for different times. $Cu_6Sn_5$ IMC layer was firstly formed in solder joints during initial soldering. If soldering at higher temperature or with a longer soldering time, $Cu_3Sn$ was produced between $Cu_6Sn_5$ and Cu due to the reaction of $Cu_6Sn_5$ and Cu. However, accompanying with the formation of $Cu_3Sn$, it was found that Bi segregation was occurred at the interface between $Cu_3Sn$ and Cu. In fact, Bi segregation was also observed during isothermal aging for Sn–58Bi solder joints. Figure 10 shows the observation by Kang et al. on Bi particles between $Cu_3Sn$ and Cu in Sn–58Bi solder joints after solid aging at 120 °C for 7 days [51]. Zou et al. [52] believed that the segregation of Bi atoms came from the Sn–Bi solder by Bi diffusion through the Cu–Sn IMC layers. Similar results were also observed by Liu et al. [14, 53]. Furthermore, Shang et al. [54] have found that Bi segregation would inevitably induce the formation of voids at the interface, as shown in Fig. 11. The authors suggested that Bi segregation acted as a barrier to Cu diffusion, and accordingly Cu atoms had to diffuse around Bi particles, creating Cu vacancies and voids in between Bi particles and Cu. The formation of voids finally

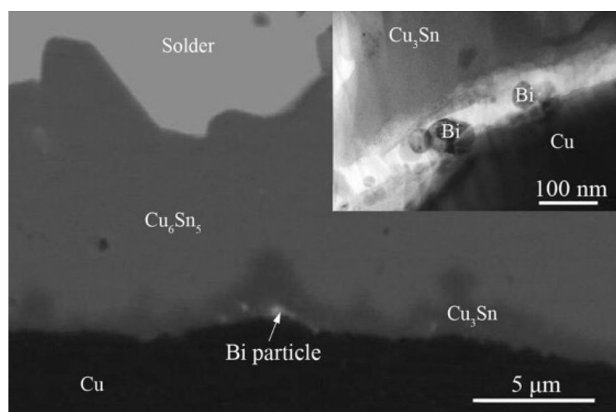


**Fig. 10** Bi segregation at $Cu_3Sn$/Cu interface in Sn–58Bi solder joint during aging [51]

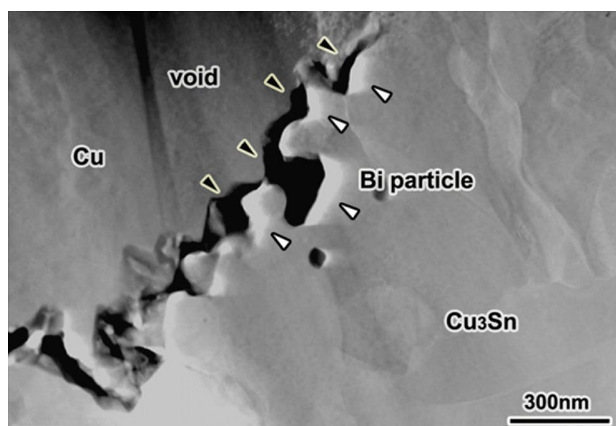


**Fig. 11** Voids induced by Bi segregation in Sn–58Bi solder joint [54]

deteriorated the fatigue resistance and tensile strength of Sn–Bi solder joints [14, 15].

To depress the IMC growth in Sn–Bi solder joints, many researchers have tried to add alloying elements into the solder. Lin et al. [55] have found that Ga addition could obviously decrease the IMC thickness in Sn–58Bi solder on Cu substrate during soldering because minor Ga addition changed the interfacial products from traditional Cu–Sn to Cu–Ga IMCs [56]. Huang and Chen [57] studied the effect of minor Co addition on the interfacial reactions in Sn–Bi/Cu couples. It was confirmed that with 0.05 or 0.5 wt% Co addition in Sn–57Bi solder the formation of $Cu_3Sn$ was completely depressed, but with increasing of Co addition the growth rate of $Cu_6Sn_5$ and the dissolution rate of Cu substrate increased. Gain and Zhang [30] studied the effect Ni nanoparticles addition on the thickness of IMC between Sn–58Bi solder and Cu substrate during soldering. It indicated that Ni addition induced the formation of $(Cu, Ni)_6Sn_5$ but prevented the formation of $Cu_3Sn$ IMC. Furthermore, the addition of 0.5 wt% Ni nanoparticles depressed the IMC growth in Sn–58Bi joints during soldering condition, as seen in Fig. 12. Mokhtari and Nishikawa [58] investigated the effect of In and Ni addition, and found that the addition of 0.5 wt% In and Ni was effective in suppressing the IMC layer growth during thermal aging. Xu et al. [59] used Sn–Ag–Cu solder to realize the depressing effect on $Cu_6Sn_5$ growth in Sn–58Bi solder joints.

Myung et al. [60] tried to investigate the effect of Ag addition and studied the IMCs between Sn–58Bi, Sn–57.6Bi–0.4Ag and Sn–57Bi–1Ag and Cu substrate during thermal aging at 85 °C. $Cu_6Sn_5$ IMCs thickness decreased due to the addition of Ag. The reason was attributed to the formation of $Ag_3Sn$ on $Cu_6Sn_5$ IMC which limited the growth of $Cu_6Sn_5$. Guan et al. [61] also found that 2 wt% Ag addition in Sn–58Bi joints depressed the IMC growth during aging at 120 °C. Shen et al. [62] studied the effect of the addition of different content from 1 to 5 wt% of Ag nano particles in Sn–30Bi–0.5Cu/Cu solder joints on IMC growth occurred in soldering condition. It was observed that the IMC growth rate in Ag-contained solders was slowed because $Ag_3Sn$ micro-particles were absorbed at the grain boundaries of Bi-rich phases and IMCs at the interface.

Mokhtari et al. [63] have investigated the effect of minor Zn addition on the IMC growth in Sn–58Bi solder joints. The content of Zn addition was selected as about 0.7 wt%. It was demonstrated that Zn addition obviously suppressed the growth of IMCs after both reflow and thermal aging. Moreover, the IMCs in Sn–Bi–Zn/Cu substrate were changed from traditional $Cu_6Sn_5$ to $Cu_5(Zn, Sn)_8$ and $Cu_6(Sn, Zn)_5$ after prolonged thermal aging. Based on Sn–58Bi–0.7Zn solder, Ma and Wu [41] furtherly studied the effect of GNSs additions with different content on IMC growth rate during liquid-state aging. Figure 13 demonstrated the interfacial structure in Sn–58Bi–0.7Zn–xGNS joints after liquid-state aging at 150 °C for 120 min. The addition of GNS could obviously depress the interfacial IMC growth. Ko et al. [64] believed that graphene accumulated at the interface hindered the diffusion of Cu atoms from the substrate and suppressed the reactions between Cu and Sn.

Many papers also found that the addition of oxides into Sn–58Bi solder was also helpful to depress the IMC growth in Sn–Bi solder joints. Liu et al. [22] have investigated the effect of $Y_2O_3$ addition, and found that with 1 wt% $Y_2O_3$ addition, the thickness of $Cu_6Sn_5$ layer and the size of the $Cu_6Sn_5$ particles reduced compared with Sn–58Bi joint because the dispersion of $Y_2O_3$ enhanced the activation energies for the growth of IMC layers. Gao et al. [65] tried to add 0.1–1.5 wt% $La_2O_3$ into Sn–58Bi solder, and found that $La_2O_3$ could restrain the segregation of Bi-rich phases.

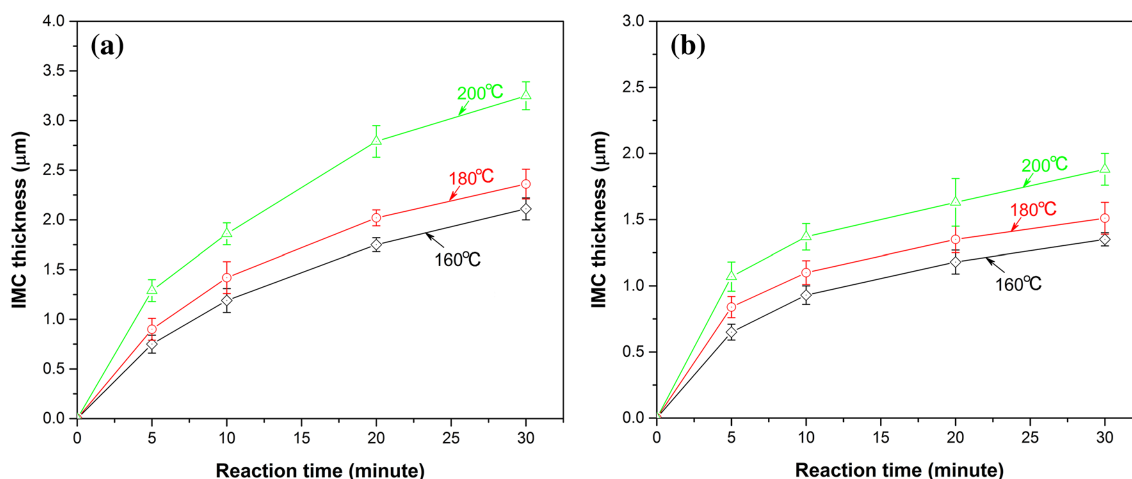


**Fig. 12** IMC layer thicknesses in **a** Sn–Bi solder and **b** Sn–Bi–0.5Ni composite solder joints on Cu substrate [30]

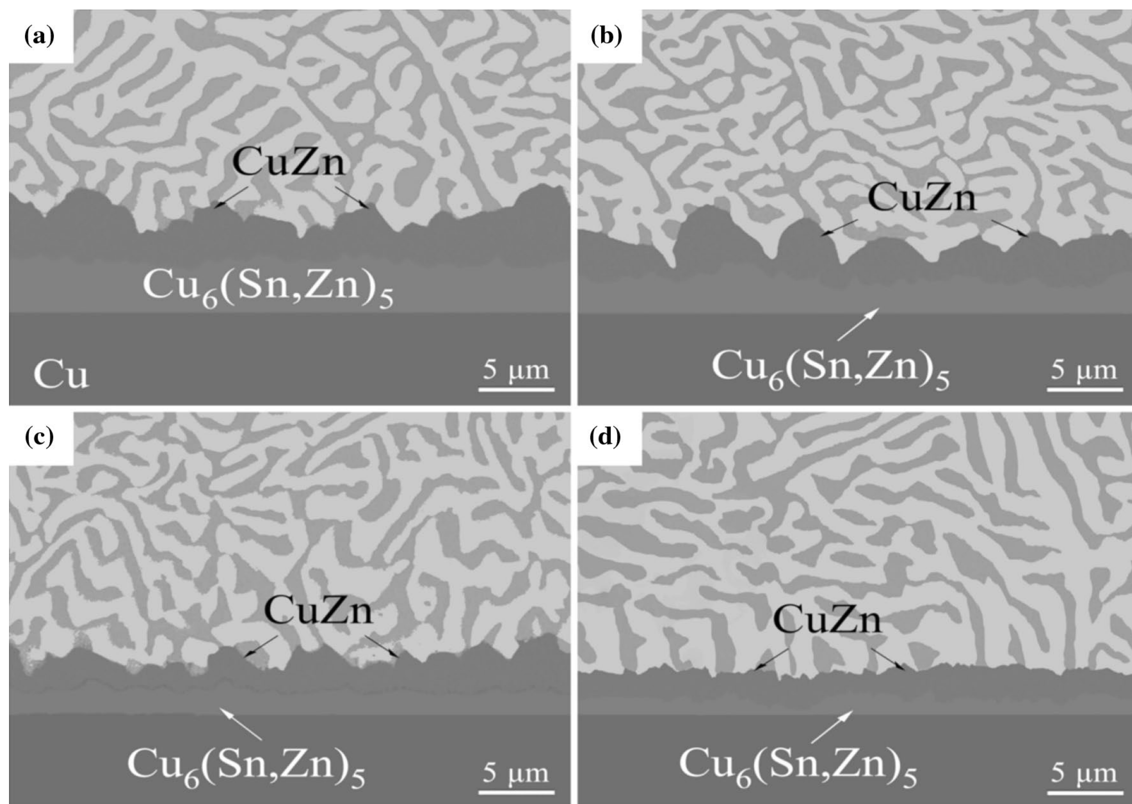


**Fig. 13** IMC layers in Sn–58Bi–0.7Zn–xGNS joints after liquid-state aging at 150 °C for 120 min: **a** 0 GNS, **b** 0.038 GNS, **c** 0.076 GNS and **d** 0.114 GNS [41]

**Table 3** IMCs in Sn–Bi solder joints bearing alloying elements

| Sn–Bi based solders/Cu | IMC growth |
|---|---|
| Sn–Bi–Ag [60, 61, 66] | The thickness of $Cu_6Sn_5$ decreased with the Ag addition. The $Ag_3Sn$ IMC was formed on $Cu_6Sn_5$ IMC which limited the growth of $Cu_6Sn_5$ |
| Sn–Bi–Co [57] | With 0.05 and 0.5 wt% Co addition in Sn–57Bi solder, the formation of $Cu_3Sn$ was completely inhibited but the growth rate of $Cu_6Sn_5$ and the dissolution rate of Cu substrate increased with Co addition |
| Sn–Bi–Cu [29] | Cu addition did not change the growth rate of interfacial IMC layer |
| Sn–Bi–Cu–Ag [62] | The Ag addition to Sn–Bi–Cu solders affected the growth rate of $Cu_6Sn_5$ IMCs |
| Sn–Bi–Ga [56] | $CuGa_2$ IMCs were produced at the interface |
| Sn–Bi–In [35] | The addition of 0.5 wt% In could suppress the IMC growth during thermal aging |
| Sn–Bi–$La_2O_3$ [65] | With $La_2O_3$ added into Sn–58Bi solder, Bi segregation was restrained, the brittleness of the solder alloy was reduced and the growth of IMC was suppressed |
| Sn–Bi–Ni [58] | A ternary scallop-shaped (Cu, Ni)–Sn IMC was produced with Ni addition. 0.5 wt% Ni addition could suppress the IMC growth during thermal aging |
| Sn–Bi–$Y_2O_3$ [22] | $Y_2O_3$ addition reduced the thickness of $Cu_6Sn_5$ layer and size of the $Cu_6Sn_5$ particles |
| Sn–Bi–Zn [63] | Zn addition suppressed the growth of IMC after both reflow and thermal aging |
| Sn–Bi–Zn–GNSs [41] | With increasing of GNSs addition, the thickness of IMC decreased |

It seems that small amount of alloying element addition was an effective way to depress the interfacial growth in Sn–Bi solder joints. Table 3 summarized the effect of alloying elements in Sn–Bi solders on IMC growth.

On the other hand, different substrates played some different effects on the evolution of interfacial IMCs, which would lead to the change of growth rate of IMCs or form different IMCs at the interface. Wang et al. [67] investigated the

interfacial reactions between Sn–Bi solders with different composition and Ni substrates at 423 K for different durations. It was indicated that only $Ni_3Sn_4$ IMC was formed at the interface. With the Bi content increased the growth rate of $Ni_3Sn_4$ IMC decreased, which was different from the growth on Cu substrate. With the aging time increased the thickness of $Ni_3Sn_4$ IMC increased. Lee et al. [68] studied the interfacial reactions between Sn–58Bi solder on organic solderability preservative (OSP), electroless nickel–immersion gold (ENIG), and electroless nickel–electroless palladium–immersion gold (ENEPIG) during soldering with different times. With OSP, the interfacial IMCs were composed of $Cu_6Sn_5$. With ENIG, the interfacial IMCs were mainly $Ni_3Sn_4$. The interfacial IMCs on the ENEPIG substrate were relatively complicated, and sequentially changed from (Pd, Ni)$Sn_4$ to (Pd, Ni)$Sn_4$ + $Ni_3Sn_4$, and then to $Ni_3Sn_4$ during soldering with different times. Furthermore, compared to the $Cu_6Sn_5$ on OSP, the $Ni_3Sn_4$ on ENIG and ENEPIG substrates were much thinner. Pun et al. [69] also studied the interfacial reaction between Sn–57Bi–1Ag solder and ENEPIG, and found that the interfacial composition was decided by the thicknesses of coated Ni(P) and Pd layers. The thin Ni(P) and Pd layers resulted in the formation of $(Ni, Cu)_3Sn_4$ instead of $Ni_3Sn_4$. It seems Bi was also not enrolled in the reaction in Sn–Bi–Ni system [70], and the results were similar as observed in Sn–Ag–Cu solder joints [71].

Chiu et al. [72] studied the interfacial reaction in Sn–Bi/Te couples. They indicated that the reaction layer was mainly composed of Sn–Te IMCs. With increasing of Bi content in Sn–Bi solders, the reaction layer became thinner. Huang et al. [45] investigated the interfacial reactions in Sn–Bi/Fe couples. The interfacial structures were shown in Fig. 14. The IMC was mainly composed of FeSn or $FeSn_2$, which was decided by the soldering temperature and time. Yen et al. [73] studied the interfacial reactions of Sn–xBi solder alloys (x = 50, 57 and 65) on Au substrate. The Au–Sn IMCs (AuSn and $AuSn_2$) and ternary Au–Bi–Sn metastable phases were formed at the interface. From Sn–Bi–Au ternary system [74], this ternary phase belonged to AuSn structure. The results also indicated that with Bi content increasing, Bi segregation was increasingly produced at the solder/Au interface.

On the other hand, alloying elements into Cu substrate was verified to be effective to eliminate Bi segregation in Sn–58Bi solder. Wang et al. [75] investigated the microstructural evolution in Sn–58Bi/Cu–Zn joints during isothermal aging. With minor Zn doped into Cu substrate, the growth of IMC layer was depressed, and the formation of $Cu_3Sn$, Kirdendall voids and Bi segregation at the interface were completely avoided, as observed in Fig. 15. Zou et al. [52, 76, 77] incorporated 2.5Ag, 8.7Ag, 10Zn or 2.3Al into Cu substrate, and similarly found that the formation of Bi segregation and voids were completely inhibited at the interface, as seen in Fig. 16.

Table 4 summarized the interfacial reaction between Sn–Bi solders on different substrates.

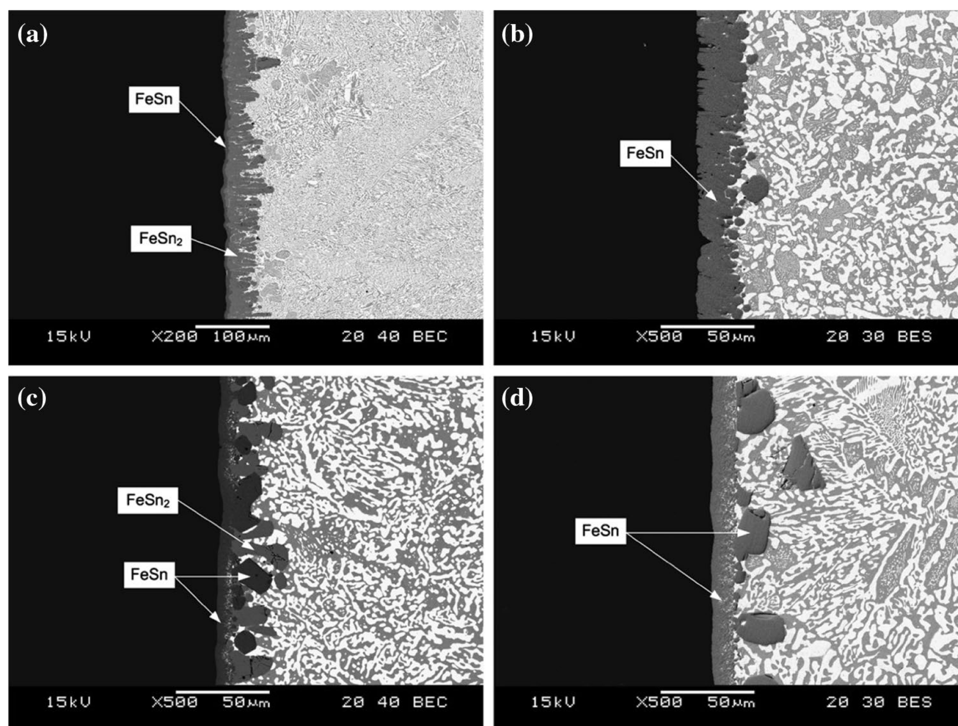


**Fig. 14** Interfacial structures in Sn–57Bi/Fe couples reacted at **a** 390 °C for 200 h, **b** 500 °C for 100 h, **c** 395 °C for 150 h, and **d** 400 °C for 200 h [45]

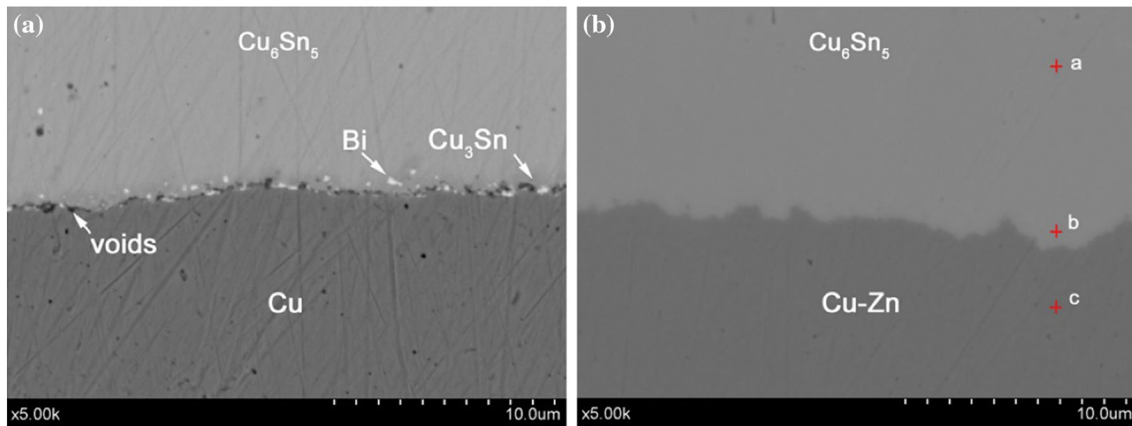


**Fig. 15** Close-up images of $Cu_6Sn_5$/substrate interface: **a** Sn–Bi/Cu and **b** Sn–Bi/Cu–Zn after aging for 60 days [75]

Bi
void
Cu
4µm
Cu2.3Al
4µm
Cu2.5Ag
2µm
Cu10Zn
4µm
Cu18.7Ag
2µm

**Fig. 16** Interfacial morphologies in aged solder joints between Sn–58Bi and different Cu substrates [52]

**Table 4** IMCs of Sn–Bi based solders reacted with different substrates

| Intermetallic compound layers | |
|---|---|
| Sn–Bi solder/substrate | |
| Sn–Bi/Cu–Ag [52, 77] | Different content of Ag was added to Cu substrate to eliminate the Bi particles and voids at the Cu/$Cu_3Sn$ interface |
| Sn–Bi/Cu–Al [52] | 2.3 wt% Al was added to Cu substrates, and Bi segregation and voids were inhibited at the Cu/$Cu_3Sn$ interface |
| Sn–Bi/Cu–Zn [75, 76] | The Kirdendall voids and Bi segregation at the interface were completely avoided in solder/Cu–Zn interface |
| Sn–Bi/ENIG [68] | $Ni_3Sn_4$ |
| Sn–Bi/ENEPIG [68, 69] | The interfacial IMCs sequentially changed from (Pd, Ni)$Sn_4$ to (Pd, Ni)$Sn_4$ + $Ni_3Sn_4$, and then to $Ni_3Sn_4$ during soldering |
| Sn–Bi/Ni [67] | $Ni_3Sn_4$ IMC was formed at the interface. The growth rate of $Ni_3Sn_4$ IMC decreased with Bi content increased |
| Sn–Bi/Fe [45] | FeSn and $FeSn_2$ IMCs were produced at the interface |
| Sn–Bi/OSP–Cu [68] | $Cu_6Sn_5$ |
| Sn–Bi/Te [72] | SnTe was produced between them. With increasing of Bi content the reaction layer became thinner |

## 5 Mechanical properties of Sn–Bi solders

### 5.1 The tensile properties

It's widely known that the tensile properties are very important to the solder alloys and their solder joints. Chen et al. [78] investigated the mechanism of Sn–58Bi solder under different temperatures and strain rates. The tensile stress–strain curves were shown in Fig. 17. It was indicated that with increasing of temperature, the tensile strength decreased while the ductility of the alloys increased. It had the opposite results with increasing of strain rate. Lai and Ye [33] studied the mechanical properties of Sn–Bi hypo eutectic solders. It was suggested that the ultimate tensile strength (UTS) and elongation of Sn–10Bi and Sn–20Bi were better than those of Sn–58Bi eutectic solder. Compared with Sn–Ag–Cu Pb free solder, Sn–Bi solder exhibited a higher tensile strength but a lower elongation [79].

Chen et al. [16] investigated the effect of In addition on the tensile properties Sn–Bi solder. It was indicated that with In addition the tensile strength of Sn–Bi solder decreased slightly, while the elongation of Sn–Bi solder increased significantly. The authors found that when the content of In reached to 2.5 wt%, the elongation of Sn–Bi solder reached the maximum with value about 44.5%. Gain and Zhang [30] studied the effect of Ni addition and compared the stress and strain behaviors of Sn–Bi and Sn–Bi–0.5Ni composite solders. It was found that the composite solder alloy had higher tensile properties than Sn–Bi solder because Ni nanoparticles was reacted with Sn to form Sn–Ni IMC particles, which were distributed in the solder matrix. Mokhtari and Nishikawa [34] investigated the effect of different content of In and Ni in Sn–58Bi-based solder. As seen in Fig. 18, it was found that the addition of 0.5 wt% Ni decreased the elongation of Sn–Bi solder because of the formation of $Ni_3Sn_4$ IMCs, while the In-bearing solders exhibited the superior elongation compared with Sn–58Bi solder because In addition promoted the formation of a large volume fraction of

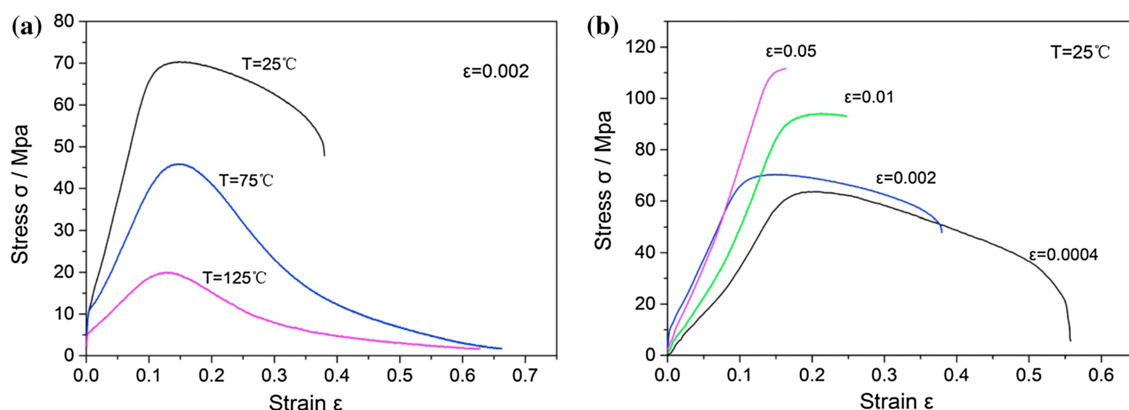


**Fig. 17** Tensile stress–strain curves of Sn–58Bi alloys: **a** stress–strain curve at different temperatures and **b** stress–strain curve at different strain rates [78]

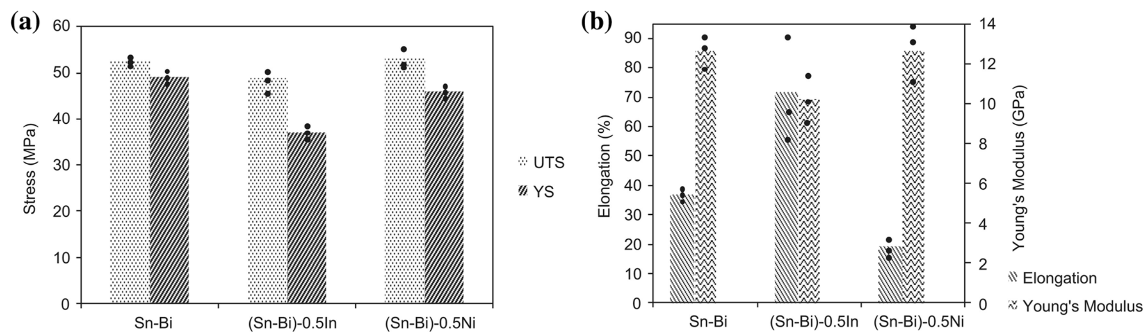


**Fig. 18** Tensile properties of In or Ni-bearing Sn–58Bi solders [34]

ductile primary Sn dendrites in the solder matrix. Chuang and Wu [36] studied the effect of Ce addition on the elongation and tensile strength of Sn–58Bi solder, it was found that Sn–58Bi–0.5Ce solder had higher elongation while lower tensile strength than Sn–58Bi solder.

The effects of minor Cu and Zn additions on tensile properties of Sn–Bi-based solders was studied by Shen et al. [38]. With the Cu and Zn addition the tensile strength increased due to the refined microstructure and the secondary particles in solder matrix, while the elongation decreased with the Zn addition due to the formation of needle-like Zn-rich phase. Ma and Wu [80] also verified that Zn addition into Sn–58Bi solder increased the UTS of the Sn–Bi solder.

Yang et al. [21] investigated the effect of $BaTiO_3$ nanoparticles on mechanical properties of Sn–58Bi solder. It was concluded that the small addition with content of 0.5–3 wt% promoted the increase on the tensile properties of Sn–Bi solder. He et al. [43] investigated the mechanical properties of Sn–58Bi alloy with addition of multi-walled CNTs (MWCNTs). It indicated that 0.03 wt% CNTs would improve the elongation and UTS of Sn–58Bi solder due to the reduction of Sn-rich segregation and the grain refinement. The increase on tensile strength from Cu-coated MWCNTs addition into Sn–30Bi solder was also confirmed by Billah and Chen [81]. The effect of GNSs on the tensile strength of Sn–58Bi–0.2Zn solder joints was studied by Ma and Wu [41], and the results showed that 0.076 wt% GNS was helpful to increase the UTS of solder join. Yang et al. [19] improved the tensile strength of Sn–58Bi solder by alloying 0.25 wt% Mo nanoparticles. Zhou et al. [44] found that 0.5Zn or 1.0Zn was helpful to improve the tensile strength of Sn–58Bi solder. Zhu et al. [82] studied the effect of $Al_2O_3$ nanoparticles on the tensile properties of Sn–58Bi solder, and found that the UTS of solder increased by 0.5 wt% addition.

As discussed above, it was concluded that the tensile properties of Sn–Bi solder were affected by the applied temperature and stain rate. Moreover, alloying elements into

**Table 5** Tensile properties of Sn–Bi based solder bearing alloying elements

| Sn–Bi based solders | Tensile properties |
|---|---|
| Sn–Bi–$Al_2O_3$ [82] | 0.5 wt% content of $Al_2O_3$ nanoparticles led to the increase on UTS |
| Sn–Bi–$BaTiO_3$ [21] | 0.5–3 wt% $BaTiO_3$ addition increased the tensile properties of Sn–58Bi solder |
| Sn–Bi–Ce [36] | 0.5Ce led to the increase on the tensile strength while the decrease on elongation |
| Sn–Bi–CNTs [43] | 0.03 wt% CNTs improved UTS and the elongation of Sn–58Bi solder |
| Sn–Bi–Cu [38] | The tensile strength and elongation increased due to Cu addition |
| Sn–Bi–In [16] | Due to In addition the tensile strength of Sn–Bi solder decreased slightly, while the elongation of Sn–Bi solder increased significantly |
| Sn–Bi–Mo [19] | 0.25 wt% Mo nanoparticles led to the increase on the tensile strength |
| Sn–Bi–Ni [30] | Ni addition increased the mechanical properties of Sn–Bi solder. 0.5 wt% Ni addition increased the elongation of solder |
| Sn–Bi–nano $Cu_6Sn_5$ [83] | 0.05 wt% $Cu_6Sn_5$ nanoparticles led to the increase on UTS |
| Sn–Bi–Zn [38, 44] | Zn addition led to the increase on the tensile strength while the decrease on elongation |
| Sn–Bi–Zn–GNSs [41] | 0.076 wt% GNSs improved the tensile strength of Sn–Bi–Zn solder |
| Sn–Bi–Zn–Al [39] | Zn–Al addition led to the increase on the fracture strain |
| Sn–Bi–Zn–P [39] | Zn–P addition led to the decrease on the fracture strain |

Sn–Bi solder also influenced the tensile properties of solder, and the related results were summarized in Table 5.

On the other hand, alloying to Cu substrate was also helpful to improve the tensile properties of Sn–58Bi solder joints. Zou et al. [15, 52, 76, 77] found that alloying Ag, Zn, Sn and Al elements into Cu substrate could significantly improve the tensile strength of Sn–58Bi solder joints even after long-term aging because of the elimination of Bi segregation and voids at the interface.

### 5.2 The shear properties

Shear test was one of common methods to evaluate the mechanical characteristics of solder ball joints. Shear fracture behaviors of Sn–58Bi/Cu solder joints were investigated by Zhang and Zhang [84]. The results showed that Sn–58Bi/Cu solder joint had good ductility under shear stress. Lee et al. [68] compared the shear force of Sn–58Bi solder on different surface finishes including OSP, ENIG and ENEPIG under three shear speeds from 0.01 to 0.5 m/s, as shown in Fig. 19, and found that ENEPIG presented the lowest strength among the joints with shorter soldering time while presented the highest strength with longer soldering time. This variation in shear force was attributed to the transition of the interfacial IMCs that formed. Moreover, the higher the shear rate was, the higher the shear was because of the increasing on the resistance to plastic deformation of solders. The fracture morphologies also verified the effect of surface finish on the shear force. On OSP and ENIG finishes, the fractures were mainly occurred in the solder matrix independent of the soldering time and shear speed, while on ENEPIG finish, the fracture was partly occurred along the interface between IMC and the solder at shorter soldering time but fully occurred in the solder matrix at longer soldering time. To improve the shear strength of Sn–58Bi solder on ENEPIG, Pun et al. [69] recommended to use a thin Ni(P) layer with thin Pd, which promoted the formation of spalling $Ni_3Sn_4$ at the interface and accordingly enhanced the joint strength. To improve the shear strength of Sn–58Bi solder on Cu substrate, Wang et al. [85] adopted Sn–3.0Ag–0.5Cu solder as the barrier layer to depress the IMC growth at the interface and to improve the shear properties of Sn–58Bi solder joints.

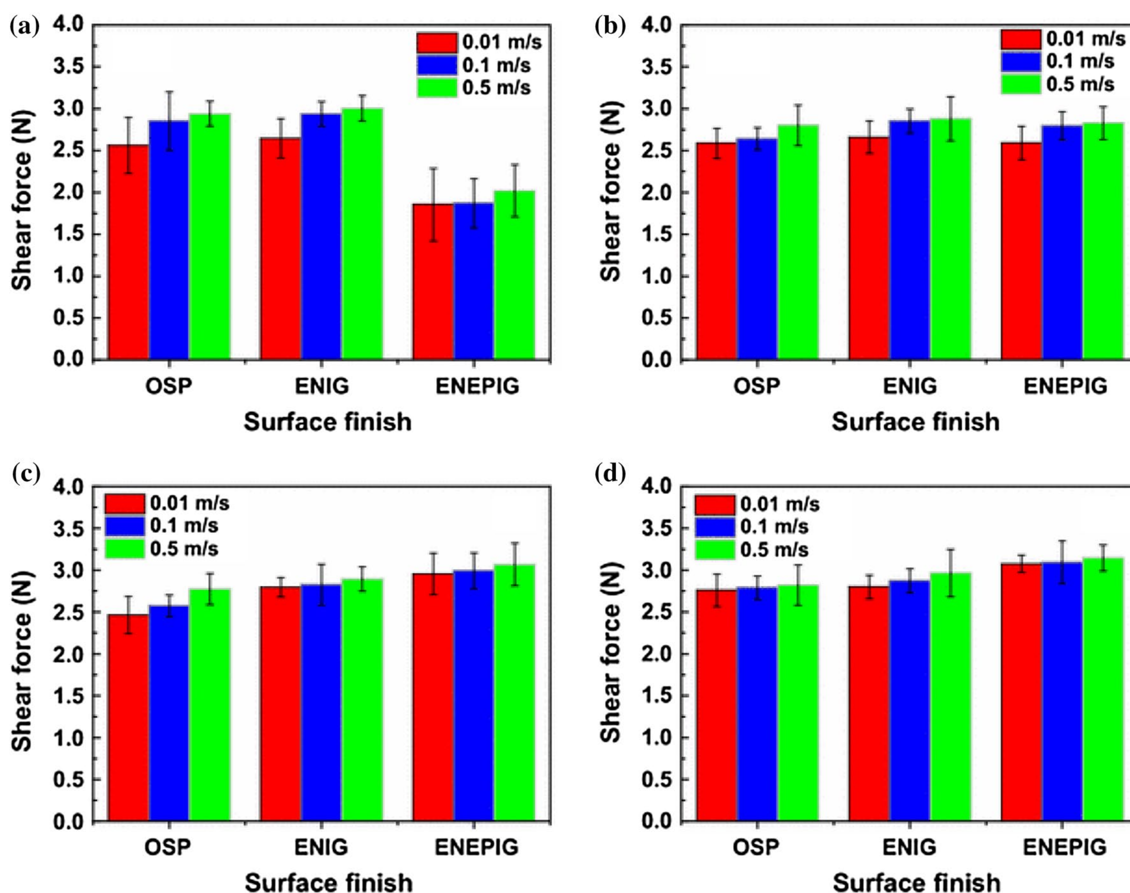


**Fig. 19** Shear force variation with surface finishes and shear speed for Sn–58Bi solder joints with different soldering times: **a** 45 s, **b** 80 s, **c** 30 min, and **d** 1 h [68]

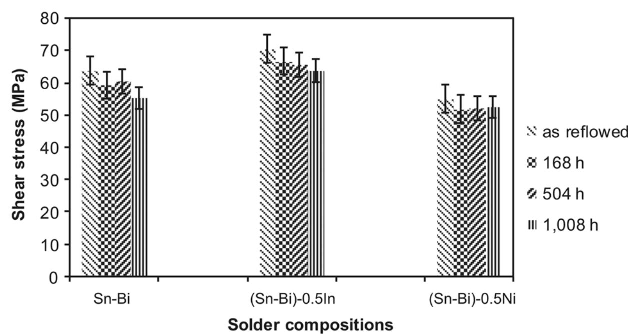


**Fig. 20** Shear test results for Sn–Bi, (Sn–Bi)–0.5In, and (Sn–Bi)–0.5Ni solder joints after reflow and thermal aging [34]

Shear force was usually affected by the aging time, temperature and the thickness of interfacial IMC layers. Mokhtari and Nishikawa [34] studied the effect of 0.5In or 0.5Ni addition on the shear properties of Sn–58Bi solder joints, and the results were given in Fig. 20. The In-bearing solder joints exhibited the greatest shear strength among all the solder joints after both reflow and thermal aging, while the addition of 0.5Ni did not alter the shear strength of Sn–Bi solder joints. The addition of In improved the shear strength of the solder joints by the refinement of the bulk Sn–Bi solder microstructure and the suppression of the brittle interfacial IMC growth. Sun et al. [86] studied the effect of the addition of 0.4 wt% Ag nanoparticles in Sn–58Bi solder (Ag-doped solder) and compared with Sn–58Bi and Sn–57.6Bi–0.4Ag (Ag-contained). The results showed that the addition of nano Ag particles could obviously improve the shear force of Sn–58Bi solder joints, i.e. Ag-doped solder exhibited the best strength for as-soldered joints, while Sn–57.6Bi–0.4Ag Ag-contained joints exhibited the best performance for as-aged joints. The reason was that $Ag_3Sn$ IMCs were gathered and the size of grains became bigger during aging condition. Zhang et al. [27] investigated the effect of Sb addition on shear properties of Sn–Bi solder joints. The shear strength decreased with Sb addition. Shen et al. [87] studied the effect of Cu, Zn on the shear properties of Sn–Bi solder. It was found that Cu addition improved the shear strength of solder while Zn addition played the deteriorated effect. In order to investigate the effect of $Y_2O_3$ particles on mechanical properties of Sn–58Bi, the shear tests were performed by Liu et al. [22]. The results showed that the shear strength increased approximately by 45% when the $Y_2O_3$ content was 1 wt%. Myung et al. [88] tried to incorporate epoxy resins into Sn–58Bi solder paste, and also found that the shear strength of the epoxy solder was about two times higher than that of Sn–Bi solder.

As discussed above, it was concluded that different alloying elements had different effects on shear strength, which were summarized in Table 6.

## 5.3 The creep properties

The high homologous temperature ($T/T_m$) at room temperature causes a large creep deformation and low creep resistance in Sn–Bi solders. Mei and Morris [13] firstly studied the creep properties of Sn–58Bi solder and compared it with Sn–37Pb solder. They found that the tested creep curve for Sn–58Bi solder followed the traditional primary, steady state and tertiary stages, and Sn–58Bi solder exhibited superior creep resistance compared with Sn–40Pb solder.

Mahmudi et al. [89] studied the creep behavior of Sn–xBi solid solution solders with Bi content ranging from 1 to 5 wt% by long time Vickers indentation testing at room temperature. It was found that the creep resistance increased with Bi content due to the strengthening effect from solid solution Bi in the Sn matrix. Shen et al. [90] furtherly studied the creep performance of Sn–Bi solders with Bi concentration ranged from 3 to 70% using nanoindentation method. Constant strain rate (CSR) method was used to extrapolate the creep stress exponent $n$ of solders. They suggested a relationship between Sn–Bi solder composition, applied stress and stress exponents or deformation mechanisms, as shown in Fig. 21. Firstly, the creep resistance decreased with the increase on Bi content in Sn–Bi solders. Compared with

**Table 6** Shear strength of Sn–Bi based solder bearing alloying elements

| Sn–Bi based solders | Shear strength |
|---|---|
| Sn–58Bi + Ag nano particles [86] | Ag nano particles were helpful to increase the shear strength of Sn–58Bi solder joints |
| Sn–57.6Bi–0.4Ag [86] | 0.4Ag was helpful to increase the strength of aged solder joints |
| Sn–Bi–Cu [87] | Cu addition would increase the shear strength |
| Sn–Bi–Cu–Zn [87] | Zn would deteriorate the shear strength of solder joints |
| Sn–Bi-epoxy [88] | The shear strength increased by 100% |
| Sn–Bi–0.5In [34] | The In-bearing solder joints exhibited higher shear strength after both reflow and thermal aging |
| Sn–Bi–Sb [27] | The shear strength decreased with Sb addition |
| Sn–Bi–$Y_2O_3$ [22] | The shear strength increased with the appropriate $Y_2O_3$ addition |

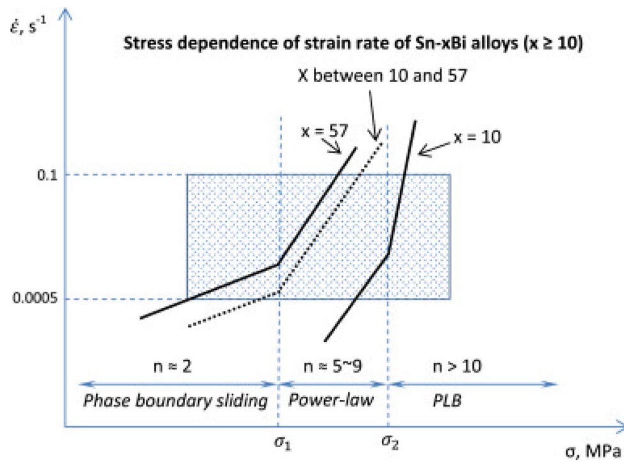


**Fig. 21** Generalized stress dependence of strain rate of Sn–xBi alloys [90]

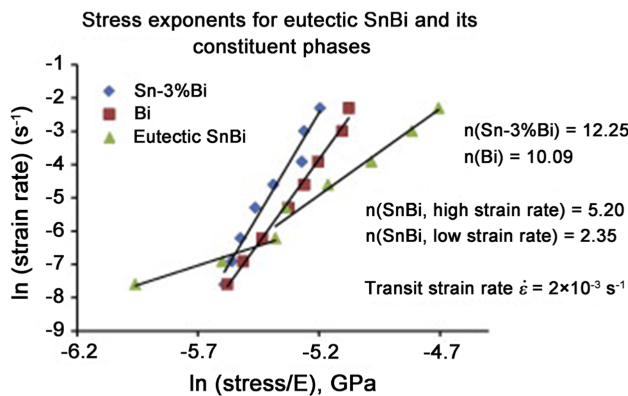


**Fig. 22** The strain rate versus the modulus compensated stress curves for β-Sn phase, Bi phase and Sn–Bi eutectic [91]

Sn–Bi solid solution solders, Sn–Bi hypoeutectic and eutectic solders presented lower creep resistance. Secondly, the creep mechanism was dependent on the applied stress and the solder composition. Dislocation glide, dislocation climb and phase boundary sliding dominated the deformation of Sn–Bi solders at the high stress region, intermediate stress region and low stress region, respectively.

Shen et al. [91] also investigated the creep deformation mechanisms on Sn–58Bi eutectic solder and its constituent phases with the results shown in Fig. 22. From the values of creep stress exponents, the power-law breakdown and grain boundary sliding were the dominant and complementary mechanisms for β-Sn and Bi phases. For Sn–58Bi eutectic solder, the dominant creep mechanism was dependent on the creep rate, i.e. grain boundary sliding at the low strain rate while dislocation climb and phase boundary sliding at the high strain rate. To obtain the activation energy $Q$ of Sn–58Bi solder, Shen et al. [92] furtherly finished the CSR tests with nanoindentation method at elevated temperatures. The calculated activation energies for β-Sn phases and Bi phases were 117.9 and 43.7 kJ/mol, while for Sn–58Bi eutectic phases were 48.2 kJ/mol at high strain rate and 55.6 kJ/mol at low strain rate, respectively. Compared with the previous results obtained by Mei and Morris [13], it presented a lower activation energy.

To improve the creep resistance of Sn–Bi solder, low concentration of Cu or Ni reactive nano-metallic fillers were added into Sn–Bi solder by Shen et al. [93]. The results showed that the creep resistance of the Sn–58Bi solder increased owing to the addition of nanometal fillers with the optimum concentrations suggested as 3 wt% for Cu and 1 wt% for Ni. The effect of RE on creep of Sn–2Bi solder was investigated by Mahmudi et al. [94]. The results indicated that 0.25RE was helpful to improve the creep resistance due to the formation of Sn–RE and Sn–Bi–RE intermetallic particles, which played a role for strengthening agent and grain refiner. Shalaby [95] studied the effect of In and Ag addition in Sn–Bi solders. It indicated that the creep rate decreased due to the addition of In and Ag, but the creep resistance of solder alloys improved.

As discussed above, it was suggested that the Bi content in Sn–Bi solder had obvious effect on the creep rate and creep resistance. Different alloying elements were also added into Sn–Bi solder to improve the creep properties, which were summarized in Table 7.

## 6 Reliabilities

The reliability of solder joints must be evaluated in electronic products. Miao et al. [96] evaluated the thermal cycling reliability on Sn–58Bi and Sn–Bi–1Cu solder joints for capacitors. There was no obvious deterioration on the joint strength after 2000 thermal cycles. Akamatsu et al.

**Table 7** Creep properties of Sn–Bi based solder bearing alloying elements

| Sn–Bi based solders | Creep properties |
| --- | --- |
| Sn–Bi–Ag [95] | The creep resistance of solder alloys improved due to the Ag addition |
| Sn–Bi–Cu [93] | 3 wt% nano Cu addition enhanced the creep resistance |
| Sn–Bi–In [95] | The creep resistance of solder alloy improved due to the In addition |
| Sn–Bi–Ni [93] | 1 wt% nano Ni addition enhanced the creep resistance |
| Sn–Bi–RE [94] | 0.25RE was helpful to improve the creep resistance of Sn–2Bi solder |

[97] also evaluated the thermal cycling reliability of ball grid array components with Sn–58Bi solder ball, and found that Sn–58Bi solder joints exhibited superior reliability compared with traditional Sn–Pb eutectic joints. Mostofizadeh et al. [98] evaluated the corrosion testing on the shear strength of eutectic Sn–Bi solder. After the salt spray test, the solder joints suffered galvanic corrosion and had a significant effect on the shear strength of the solder joints.

However, due to the embrittlement of Bi element, the serious problem on Sn–Bi solder joints was their poor drop reliability. Therefore, the work on reliability of Sn–58Bi solder joints is how to improve the drop performance. Myung et al. [88] have studied the effect of epoxy resins in Sn–58Bi solder paste on the drop reliability at bare Cu and OSP-Cu substrates. The comparison on Weibull probability distribution and average number of drops between Sn–58Bi solder and epoxy solder were plotted in Fig. 23. It can be observed that most of Sn–58Bi solder joints were failed in 10 drops, while the drop numbers on Sn–58Bi epoxy solder joints were reached with about 100–200. Lee et al. [99] further investigated the drop reliability of Sn–58Bi epoxy solder on ENIG and ENEPIG pads, and found that their drop reliability was poorer than that on OSP. Therefore, the authors suggested that ENIG and ENEPIG should be carefully selected for Sn–58Bi epoxy solder. The similar compared results were also verified in [100].

Besides the drop reliability, electromigration has been gotten much attention for Sn–58Bi solder joints in recent years. It is the mass transport of atom driven by combined forces of electric wind. Accordingly, phase separation was likely to occur under electromigration due to the different atomic diffusivities. Figure 24 shows Bi accumulation at anode side in Sn–58Bi joint under the current $5 \times 10^3$ A/cm$^2$ at 75 °C [101]. Moreover, Gu et al. [102, 103] used

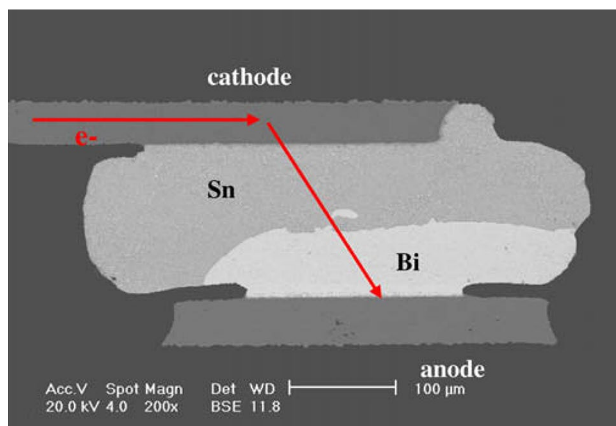


**Fig. 24** SEM image on Bi accumulation in Sn–58Bi solder joint under a current density of $5 \times 10^3$ A/cm$^2$ at 75 °C [101]

the line-type Sn–58Bi solder joints to study the atomic migration under electromigration, and observed the formation of Bi-rich layer at the anode side. Its thickness increased with applied current density and temperature [104].

The formation of Bi-rich layer would accelerate the formation of voids and cracks at the anode, and finally deteriorated the joint strength of Sn–Bi solder joints [105]. Therefore, one of the methods to improve Sn–Bi solder joints under electromigration was to depress the formation of Bi-rich layer by alloying elements into solder. The additions of RE by He et al. [106], nano $Al_2O_3$ particles by Hu et al. [107, 108], Ag element or Ag nanoparticles by Ismathullakhan and Li et al. [40, 109], GNSs by Ma and Wu [110], micro Ni particles by Xu et al. [111], Ge by Zhao et al. [112] and Sn–3.0Ag–0.5Cu interlayer by Wang et al. [113] have been verified to inhibit the diffusion of Bi atoms under current stressing.

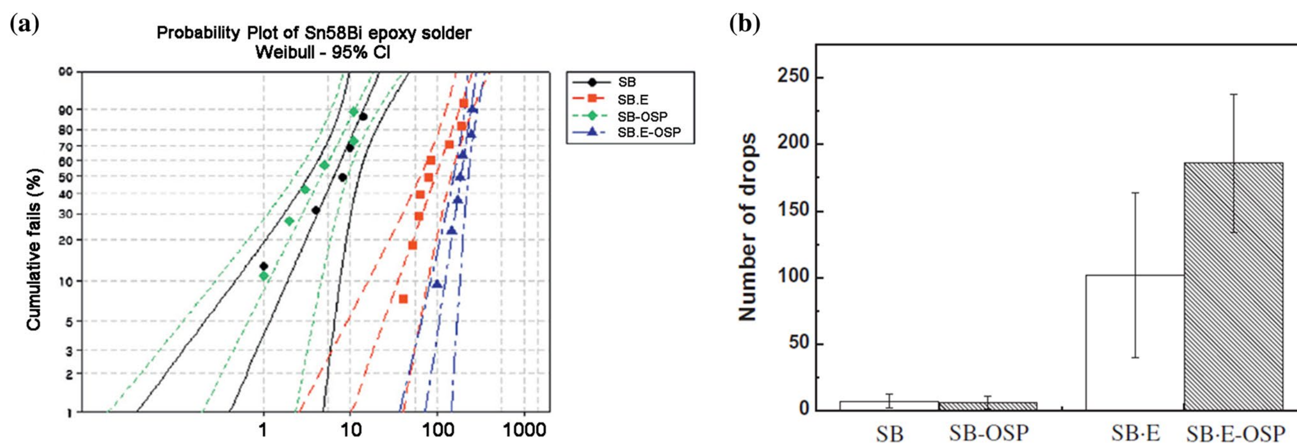


**Fig. 23** Drop results on Sn–58Bi epoxy solder: **a** Weibull probability distribution and **b** average number of drops [88]

## 7 Conclusions

With the strengthening of people's awareness of environmental protection, Sn–Ag–Cu series solder has been widely used to replace traditional Sn–Pb solder in electronic industry. However, under the motivation on low temperature soldering from technical, reliability and economic issues, Sn–Bi based Pb-free solders have been gotten much attention to be the promising candidates which met the requirements for low melting point, low cost and environment friendly. However, the disadvantage of brittleness characteristic and prone to coarsening at high temperature prevented its wide practical application. In order to promote the better application of Sn–Bi based solders in electronic industry, many efforts have been made to improve the wettability, mechanical properties and reliability of Sn–Bi based solders. According to the existing research results, it provides an important basis of understanding the current development of Sn–Bi solders. With the purpose of further improve the properties of Sn–Bi solders, there still exists some technical problems caused from the existence of Bi addition to be solved for Sn–Bi solders:

(1) Due to the inherent brittleness of Bi element, there exists a high risk of brittle fracture of Sn–Bi based solder joints under mechanical shock and drop conditions for electronic products. Currently, there are less achievements on the development of more ductile Sn–Bi solder although many researchers have tried to reduce the Bi content and incorporate the elemental dopants.
(2) *Interfacial issues* the formation of Bi segregation and Bi-rich layer and over growth of interfacial IMC layer are easily occurred in Sn–Bi solder joints during service condition, which seriously deteriorates the performance of Sn–Bi solder joints.
(3) There are fewer works on the reliability of Sn–Bi solder joints such as thermal cycling, mechanical vibration, etc. The reliability of Sn–Bi solder joints should be systematically evaluated.

**Acknowledgements** The authors would like to acknowledge the support provided by the National Natural Science Foundation of China (Grant No. 51875269) and the Postgraduate Research and Practice Innovation Program of Jiangsu Province (Grant Nos. SJCX18_0760 and KYCX17_1835).

### Compliance with ethical standards

**Conflict of interest** No.

## References

1. K.N. Tu, K. Zeng, Tin–lead (SnPb) solder reaction in flip chip technology. Mater. Sci. Eng. R **34**, 1–58 (2001)
2. L. Zhang, K.N. Tu, Structure and properties of lead-free solders bearing micro and nano particles. Mater. Sci. Eng. R **82**, 1–32 (2014)
3. I.E. Anderson, Development of Sn–Ag–Cu and Sn–Ag–Cu–X alloys for Pb-free electronic solder applications. J. Mater. Sci. Mater. Electron. **18**, 55–76 (2007)
4. H. Ma, J.C. Suhling, A review of mechanical properties of lead-free solders for electronic packaging. J. Mater. Sci. **44**, 1141–1158 (2009)
5. D. Amir, S. Walwadkar, S. Aravamudhan, L. May, in *The Challenges of Non-wet Open BGA Solder Defect*. SMTAI Proceedings, Orlando, FL, 2012, pp. 684–694
6. B. Sandy, E. Briggs, R. Lasky, Advantages of bismuth-based alloys for low-temperature lead-free soldering and rework. Surf. Mt Technol. Mag. **26**, 26–40 (2011)
7. Z. Zhao, C. Chen, C.Y. Park, Y. Wang, L. Liu, G. Zou, J. Cai, Q. Wang, Effects of package warpage on Head-in-Pillow defect. Mater. Trans. **56**, 1037–1042 (2015)
8. K. Suganuma, K. Niihara, T. Shoutoku, Y. Nakamura, Wetting and interface microstructure between Sn–Zn binary alloys and Cu. J. Mater. Res. **13**, 2859–2865 (1998)
9. S. Liu, S.B. Xue, P. Xue, D.X. Luo, Present status of Sn–Zn lead-free solders bearing alloying elements. J. Mater. Sci. Mater. Electron. **26**, 4389–4411 (2015)
10. H.R. Kotadia, P.D. Howes, S.H. Mannan, A review: on the development of low melting temperature Pb-free solders. Microelectron. Reliab. **54**, 1253–1273 (2014)
11. Y. Li, F.S. Wu, Y.C. Chan, Electromigration in eutectic In–48Sn ball grid array (BGA) solder interconnections with Au/Ni/Cu pads. J. Mater. Sci. Mater. Electron. **26**, 8522–8533 (2015)
12. F. Hua, Z. Mei, J. Glazer, in *Eutectic Sn–Bi as an Alternative to Pb-Free Solders*. 48th Electronic Components and Technology Conference, Seattle, WA, 1998, pp. 277–283
13. Z. Mei, J.W. Morris, Characterization of eutectic Sn–Bi solder joints. J. Electron. Mater. **21**, 599–607 (1992)
14. P.L. Liu, J.K. Shang, Interfacial embrittlement by bismuth segregation copper/tin–bismuth Pb-free solder interconnect. J. Mater. Res. **16**, 1651–1659 (2001)
15. H.F. Zou, Q.K. Zhang, Z.F. Zhang, Transition of Bi embrittlement of SnBi/Cu joint couples with reflow temperature. J. Mater. Res. **26**, 449–454 (2010)
16. X. Chen, F. Xue, J. Zhou, Y. Yao, Effect of In on microstructure, thermodynamic characteristic and mechanical properties of Sn–Bi based lead-free solder. J. Alloy Compd **633**, 377–383 (2015)
17. W.X. Dong, Y.W. Shi, Z.D. Xia, Y.P. Lei, F. Guo, Effects of trace amounts of rare earth additions on microstructure and properties of Sn–Bi-based solder alloy. J. Electron. Mater. **37**, 982–991 (2008)
18. A.K. Gain, L. Zhang, Interfacial microstructure, wettability and material properties of nickel (Ni) nanoparticle doped tin–bismuth–silver (Sn–Bi–Ag) solder on copper (Cu) substrate. J. Mater. Sci. Mater. Electron. **27**, 3982–3994 (2016)
19. L. Yang, L. Zhu, Y.C. Zhang, P. Liu, N. Zhang, S.Y. Zhou, L.C. Jiang, Microstructure and reliability of Mo nanoparticle reinforced Sn–58Bi-based lead-free solder joints. Mater. Sci. Technol. **34**, 992–1002 (2018)
20. Y. Liu, H. Zhang, F.L. Sun, Solderability of SnBi-nano Cu solder pastes and microstructure of the solder joints. J. Mater. Sci. Mater. Electron. **27**, 2235–2241 (2016)
21. L. Yang, J. Dai, Y.C. Zhang, Y.F. Jing, J.G. Ge, H.X. Liu, Influence of $BaTiO_3$ nanoparticle addition on microstructure and

mechanical properties of Sn–58Bi solder. J. Electron. Mater. **44**, 2473–2478 (2015)
22. X.Y. Liu, M.L. Huang, C.M.L. Wu, L. Wang, Effect of $Y_2O_3$ particles on microstructure formation and shear properties of Sn–58Bi solder. J. Mater. Sci. Mater. Electron. **21**, 1046–1054 (2010)
23. L. Yang, C.C. Du, J. Dai, N. Zhang, Y.F. Jing, Effect of nano-sized graphite on properties of Sn–Bi solder. J. Mater. Sci. Mater. Electron. **24**, 4180–4185 (2013)
24. S.T. Oh, J.H. Lee, Microstructural, wetting, and mechanical characteristics of Sn–57.6Bi–0.4Ag alloys doped with metal-organic compounds. Electron. Mater. Lett. **10**, 473–478 (2014)
25. C.-B. Lee, S.-B. Jung, Y.-E. Shin, C.-C. Shur, The effect of Bi concentration on wettability of Cu substrate by Sn–Bi solders. Mater. Trans. **42**, 751–755 (2001)
26. X. Chen, F. Xue, J. Zhou, S. Liu, G. Qian, Microstructure, thermal and wetting properties of Sn–Bi–Zn lead-free solder. J. Electron. Mater. **42**, 2708–2715 (2013)
27. C. Zhang, S. Liu, G. Qian, J. Zhou, F. Xue, Effect of Sb content on properties of Sn–Bi solders. Trans. Nonferr. Met. Soc. China **24**, 184–191 (2014)
28. P. Sebo, P. Svec, D. Janickovic, E. Illekova, M. Zemankova, Y. Plevachuk, V. Sidorov, P. Svec, The influence of silver content on structure and properties of Sn–Bi–Ag solder and Cu/solder/Cu joints. Mater. Sci. Eng. A **571**, 184–192 (2013)
29. Z.M. Lai, D. Ye, Microstructure and properties of Sn–10Bi–xCu solder alloy/joint. J. Electron. Mater. **45**, 3702–3711 (2016)
30. A.K. Gain, L.C. Zhang, Growth mechanism of intermetallic compound and mechanical properties of nickel (Ni) nanoparticle doped low melting temperature tin–bismuth (Sn–Bi) solder. J. Mater. Sci. Mater. Electron. **27**, 781–794 (2016)
31. S.A. Belyakov, C.M. Gourlay, Recommended values for the β-Sn solidus line in Sn–Bi alloys. Thermochim. Acta **654**, 65–69 (2017)
32. F. Wang, Y. Huang, Z. Zhang, C. Yan, Interfacial reaction and mechanical properties of Sn–Bi solder joints. Materials **10**(8), 920 (2017)
33. Z.M. Lai, D. Ye, Microstructure and fracture behavior of non eutectic Sn–Bi solder alloys. J. Mater. Sci. Mater. Electron. **27**, 3182–3192 (2016)
34. O. Mokhtari, H. Nishikawa, Correlation between microstructure and mechanical properties of Sn–Bi–X solders. Mater. Sci. Eng. A **651**, 831–839 (2016)
35. Q. Li, N. Ma, Y. Lei, J. Lin, H. Fu, J. Gu, Characterization of low-melting-point Sn–Bi–In lead-free solders. J. Electron. Mater. **45**, 5800–5810 (2016)
36. T.-H. Chuang, H.-F. Wu, Effects of Ce addition on the microstructure and mechanical properties of Sn–58Bi solder joints. J. Electron. Mater. **40**, 71–77 (2011)
37. J. Shen, C. Wu, S. Li, Effects of rare earth additions on the microstructural evolution and microhardness of Sn30Bi0.5Cu and Sn35Bi1Ag solder alloys. J. Mater. Sci. Mater. Electron. **23**, 156–163 (2012)
38. J. Shen, Y.Y. Pu, H.G. Yin, D.J. Luo, J. Chen, Effects of minor Cu and Zn additions on the thermal, microstructure and tensile properties of Sn–Bi-based solder alloys. J. Alloy Compd **614**, 63–70 (2014)
39. X.J. Wang, Y.L. Wang, F. Wang, N. Liu, J.X. Wang, Effects of Zn, Zn–Al and Zn–P additions on the tensile properties of Sn–Bi solder. Acta Metall. Sin. Engl. Lett. **27**, 1159–1164 (2014)
40. Y. Li, K.M. Luo, A.B.Y. Lim, Z. Chen, F.S. Wu, Y.C. Chan, Improving the mechanical performance of Sn57.6Bi0.4Ag solder joints on Au/Ni/Cu pads during aging and electromigration through the addition of tungsten (W) nanoparticle reinforcement. Mater. Sci. Eng. A **669**, 291–303 (2016)
41. D.L. Ma, P. Wu, Improved microstructure and mechanical properties for Sn58Bi0.7Zn solder joint by addition of graphene nanosheets. J. Alloy Compd **671**, 127–136 (2016)
42. Y. Ma, X. Li, W. Zhou, L. Yang, P. Wu, Reinforcement of graphene nanosheets on the microstructure and properties of Sn58Bi lead-free solder. Mater. Des. **113**, 264–272 (2017)
43. P. He, X.C. Lu, T.S. Lin, H.X. Li, J. An, X. Ma, J.C. Feng, Y. Zhang, Q. Li, Y.Y. Qian, Improvement of mechanical properties of Sn–58Bi alloy with multi-walled carbon nanotubes. Trans. Nonferr. Met. Soc. China **22**, S692–S696 (2012)
44. S. Zhou, O. Mokhtari, M.G. Rafique, V.C. Shunmugasamy, B. Mansoor, H. Nishikawa, Improvement in the mechanical properties of eutectic Sn58Bi alloy by 0.5 and 1 wt% Zn addition before and after thermal aging. J. Alloy Compd **765**, 1243–1252 (2018)
45. Y.C. Huang, W. Gierlotka, S.W. Chen, Sn–Bi–Fe thermodynamic modeling and Sn–Bi/Fe interfacial reactions. Intermetallics **18**, 984–991 (2010)
46. M. Hirman, K. Rendl, F. Steiner, V. Wirth, in *Influence of Reflow Soldering Profiles on Creation of IMC at the Interface of SnBi/Cu*. 37th International Spring Seminar on Electronics Technology, 2014, pp. 147–151
47. T.Y. Kang, Y.Y. Xiu, L. Hui, J.J. Wang, W.P. Tong, C.Z. Liu, Effect of bismuth on intermetallic compound growth in lead free solder/Cu microelectronic interconnect. J. Mater. Sci. Technol. **27**, 741–745 (2011)
48. F. Wang, H. Chen, Y. Huang, C. Yan, Interfacial behavior and joint strength of Sn–Bi solder with solid solution compositions. J. Mater. Sci. Mater. Electron. **29**, 11409–11420 (2018)
49. T. Laurila, V. Vuorinen, J.K. Kivilahti, Interfacial reactions between lead-free solders and common base materials. Mater. Sci. Eng. R **49**, 1–60 (2005)
50. X. Hu, Y. Li, Z. Min, Interfacial reaction and growth behavior of IMCs layer between Sn–58Bi solders and a Cu substrate. J. Mater. Sci. Mater. Electron. **24**, 2027–2034 (2013)
51. T.Y. Kang, Y.Y. Xiu, C.Z. Liu, L. Hui, J.J. Wang, W.P. Tong, Bismuth segregation enhances intermetallic compound growth in SnBi/Cu microelectronic interconnect. J. Alloy Compd **509**, 1785–1789 (2011)
52. H.F. Zou, Q.K. Zhang, Z.F. Zhang, Interfacial microstructure and mechanical properties of SnBi/Cu joints by alloying Cu substrate. Mater. Sci. Eng. A **532**, 167–177 (2012)
53. C.Z. Liu, W. Zhang, Bismuth redistribution induced by intermetallic compound growth in SnBi/Cu microelectronic interconnect. J. Mater. Sci. **2009**, 149–153 (2009)
54. P.J. Shang, Z.Q. Liu, D.X. Li, J.K. Shang, Bi-induced voids at the Cu3Sn/Cu interface in eutectic SnBi/Cu solder joints. Scr. Mater. **58**, 409–412 (2008)
55. S.-K. Lin, T.L. Nguyen, S.-C. Wu, Y.-H. Wang, Effective suppression of interfacial intermetallic compound growth between Sn–58 wt.% Bi solders and Cu substrates by minor Ga addition. J. Alloy Compd **586**, 319–327 (2014)
56. C.H. Chen, B.H. Lee, H.C. Chen, C.M. Wang, A.T. Wu, Interfacial reactions of low-melting Sn–Bi–Ga solder alloy on Cu substrate. J. Electron. Mater. **45**, 197–202 (2016)
57. Y.-C. Huang, S.-W. Chen, Effects of Co alloying and size on solidification and interfacial reactions in Sn–57 wt.% Bi–(Co)/Cu couples. J. Electron. Mater. **40**, 62–70 (2011)
58. O. Mokhtari, H. Nishikawa, Effects of In and Ni addition on microstructure of Sn–58Bi solder joint. J. Electron. Mater. **43**, 4158–4170 (2014)
59. R. Xu, Y. Liu, H. Zhang, Z. Li, F. Sun, G. Zhang, Evolution of the microstructure of Sn58Bi solder paste with Sn–3.0Ag–0.5Cu addition during isothermal aging. J. Electron. Mater. (2018). https://doi.org/10.1007/s11664-018-06865-1

60. W.R. Myung, M.K. Ko, Y. Kim, S.B. Jung, Effects of Ag content on the reliability of LED package component with Sn–Bi–Ag solder. J. Mater. Sci. Mater. Electron. **26**, 8707–8713 (2015)
61. Z.-M. Guan, G.-X. Liu, T. Liu, Kinetics of interface reaction in 40Sn–Bi/Cu and 40Sn–Bi–2Ag/Cu systems during aging in solid state. IEEE Trans. Adv. Packag. **23**, 737–742 (2000)
62. J. Shen, C.F. Peng, M.L. Zhao, C.P. Wu, Microstructural evolutions of the Ag nano-particle reinforced SnBiCu–xAg/Cu solder joints during liquid aging. J. Mater. Sci. Mater. Electron. **23**, 1409–1414 (2012)
63. O. Mokhtari, S. Zhou, Y.C. Chan, H. Nishikawa, Effect of Zn addition on interfacial reactions between Sn–Bi solder and Cu substrate. Mater. Trans. **57**, 1272–1276 (2016)
64. Y.-H. Ko, J.-D. Lee, T. Yoon, C.-W. Lee, T.-S. Kim, Controlling interfacial reactions and intermetallic compound growth at the interface of a lead-free solder joint with layer-by-layer transferred graphene. ACS Appl. Mater. Interfaces **8**, 5679–5686 (2016)
65. L. Gao, J. Wang, T. Lin, P. He, F. Lu, in *Improvement of Microstructure and Mechanical Properties of Sn–58Bi Alloy with* $La_2O_3$. 14th International Conference on Electronic Packaging Technology, 2013, pp. 193–195
66. K. Suganuma, T. Sakai, K.-S. Kim, Y. Takagi, J. Sugimoto, M. Ueshima, Thermal and mechanical stability of soldering QFP with Sn–Bi–Ag lead-free alloy. IEEE Trans. Electron. Packag. Manuf. **25**(4), 257–261 (2002)
67. J. Wang, H.S. Liu, L.B. Liu, Z.P. Jin, Interfacial reaction between Sn–Bi alloy and Ni substrate. J. Electron. Mater. **35**, 1842–1847 (2006)
68. S.-M. Lee, J.-W. Yoon, S.-B. Jung, Interfacial reaction and mechanical properties between low melting temperature Sn–58Bi solder and various surface finishes during reflow reactions. J. Mater. Sci. Mater. Electron. **26**, 1649–1660 (2015)
69. K.P.L. Pun, M.N. Islam, J. Rotanson, C.-W. Cheung, A.H.S. Chan, Enhancement of Sn–Bi–Ag solder Joints with ENEPIG surface finish for low-temperature interconnection. J. Electron. Mater. **47**, 5191–5202 (2018)
70. G.P. Vassilev, K.I. Lilova, J.C. Gachon, Phase diagram investigations of the Ni–Sn–Bi system. J. Alloy Compd **469**, 264–269 (2009)
71. Z. Zhang, X. Hu, X. Jiang, Y. Li, Influences of mono-Ni(P) and dual-Cu/Ni(P) plating on the interfacial microstructure evolution of solder joints. Metall. Mater. Trans. A (2018). https://doi.org/10.1007/s11661-018-4983-7
72. C.N. Chiu, C.H. Wang, S.W. Chen, Interfacial reactions in the Sn–Bi/Te couples. J. Electron. Mater. **37**, 40–44 (2008)
73. Y.W. Yen, W.K. Liou, C.M. Chen, C.K. Lin, M.K. Huang, Interfacial reactions in the Sn–xBi/Au couples. Mater. Chem. Phys. **128**, 233–237 (2011)
74. F. Gao, C. Wang, X. Liu, Y. Takaku, I. Ohnuma, K. Ishida, Thermodynamic assessment of phase equilibria in the Sn–Au–Bi system with key experimental verification. J. Mater. Res. **25**(3), 576–586 (2010)
75. F. Wang, L. Zhou, X. Wang, P. He, Microstructural evolution and joint strength of Sn–58Bi/Cu joints through minor Zn alloying substrate during isothermal aging. J. Alloy Compd **688**, 639–648 (2016)
76. Q.K. Zhang, H.F. Zou, Z.F. Zhang, Improving tensile and fatigue properties of Sn–58Bi/Cu solder joints through alloying substrate. J. Mater. Res. **25**, 303–314 (2010)
77. Q.K. Zhang, H.F. Zou, Z.F. Zhang, Influences of substrate alloying and reflow temperature on Bi segregation behaviors at Sn–Bi/Cu interface. J. Electron. Mater. **40**(11), 2320–2328 (2011)
78. X. Chen, J. Zhou, F. Xue, Y. Yao, Mechanical deformation behavior and mechanism of Sn–58Bi solder alloys under different temperatures and strain rates. Mater. Sci. Eng. A **662**, 251–257 (2016)
79. I. Abdullah, M.N. Zulkifli, A. Jalar, R. Ismail, Deformation behaviour of Sn–3.0Ag–0.5Cu (SAC305) solder wire under varied tensile strain rates. Solder. Surf. Mt Technol. **29**, 110–117 (2017)
80. D.L. Ma, P. Wu, Effects of Zn addition on mechanical properties of eutectic Sn–58Bi solder during liquid-state aging. Trans. Nonferr. Met. Soc. China **25**(4), 1225–1233 (2015)
81. M.M. Billah, Q. Chen, Strength of MWCNT-reinforced 70Sn–30Bi solder alloys. J. Electron. Mater. **45**, 98–103 (2016)
82. W.B. Zhu, Y. Ma, X.Z. Li, W. Zhou, P. Wu, Effects of $Al_2O_3$ nanoparticles on the microstructure and properties of Sn58Bi solder alloys. J. Mater. Sci. Mater. Electron. **29**, 7575–7585 (2018)
83. X.Z. Li, Y. Ma, W. Zhou, P. Wu, Effects of nanoscale $Cu_6Sn_5$ particles addition on microstructure and properties of SnBi solder alloys. Mater. Sci. Eng. A **684**, 328–334 (2017)
84. Q.K. Zhang, Z.F. Zhang, In situ observations on shear and creep–fatigue fracture behaviors of SnBi/Cu solder joints. Mater. Sci. Eng. A **528**, 2686–2693 (2011)
85. F. Wang, D. Li, Z. Zhang, M. Wu, C. Yan, Improvement on interfacial structure and properties of Sn–58Bi/Cu joint using Sn–3.0Ag–0.5Cu solder as barrier. J. Mater. Sci. Mater. Electron. **28**, 19051–19060 (2017)
86. H.Y. Sun, Q.Q. Li, Y.C. Chan, A study of Ag additive methods by comparing mechanical properties between Sn57.6Bi0.4Ag and 0.4 wt% nano-Ag-doped Sn58Bi BGA solder joints. J. Mater. Sci. Mater. Electron. **25**, 4380–4390 (2014)
87. J. Shen, Y.Y. Pu, H.G. Yin, Q. Tang, Effects of Cu, Zn on the wettability and shear mechanical properties of Sn–Bi-based lead-free solders. J. Electron. Mater. **44**, 532–541 (2015)
88. W.-R. Myung, Y. Kim, S.-B. Jung, Mechanical property of the epoxy-contained Sn–58Bi solder with OSP surface finish. J. Alloy Compd **615**, S411–S417 (2014)
89. R. Mahmudi, A.R. Geranmayeh, S.R. Mahmoodi, A. Khalatbari, Room-temperature indentation creep of lead-free Sn–Bi solder alloys. J. Mater. Sci. Mater. Electron. **18**, 1071–1078 (2007)
90. L. Shen, P. Septiwerdani, Z. Chen, Elastic modulus, hardness and creep performance of SnBi alloys using nanoindentation. Mater. Sci. Eng. A **558**, 253–258 (2012)
91. L. Shen, P. Lu, S. Wang, Z. Chen, Creep behaviour of eutectic SnBi alloy and its constituent phases using nanoindentation technique. J. Alloys Compd **574**, 98–103 (2013)
92. L. Shen, Y. Wu, S. Wang, Z. Chen, Creep behavior of Sn–Bi solder alloys at elevated temperatures studied by nanoindentation. J. Mater. Sci. Mater. Electron. **28**, 4114–4124 (2017)
93. L. Shen, Z.Y. Tan, Z. Chen, Nanoindentation study on the creep resistance of SnBi solder alloy with reactive nano-metallic fillers. Mater. Sci. Eng. A **561**, 232–238 (2013)
94. R. Mahmudi, A.R. Geranmayeh, M. Salehi, H. Pirayesh, Impression creep of the rare-earth doped Sn–2% Bi lead-free solder alloy. J. Mater. Sci. Mater. Electron. **21**, 262–269 (2010)
95. R.M. Shalaby, Effect of silver and indium addition on mechanical properties and indentation creep behavior of rapidly solidified Bi–Sn based lead-free solder alloys. Mater. Sci. Eng. A **560**, 86–95 (2013)
96. H.-W. Miao, J.-G. Duh, B.-S. Chiou, Thermal cycling test in Sn–Bi and Sn–Bi–Cu solder joints. J. Mater. Sci. Mater. Electron. **11**, 609–618 (2000)
97. T. Akamatsu, Y. Yamagishi, K. Imamura, O. Yamaguchi, M. Minamizawa, in *Solder Joint Reliability of BGA Package with Sn–Bi System Solder Balls*. Proceedings of SPIE—The International Society for Optical Engineering, vol. 4587, 2001, pp. 547–552
98. M. Mostofizadeh, J. Pippola, L. Frisk, Shear strength of eutectic Sn–Bi lead-free solders after corrosion testing and thermal aging. J. Electron. Mater. **43**, 1335–1346 (2014)

99. S.-M. Lee, J.-W. Yoon, S.-B. Jung, Board level drop reliability of epoxy-containing Sn–58 mass% Bi solder joints with various surface finishes. Mater. Trans. **57**, 466–471 (2016)
100. W.-R. Myung, Y. Kim, S.-B. Jung, Evaluation of the bondability of the epoxy-enhanced Sn–58Bi solder with ENIG and ENEPIG surface finishes. J. Electron. Mater. **44**, 4637–4645 (2015)
101. Y.C. Chan, D. Yang, Failure mechanisms of solder interconnects under current stressing in advanced electronic packages. Prog. Mater. Sci. **55**, 428–475 (2010)
102. X. Gu, Y.C. Chan, Electromigration in line-type Cu/Sn–Bi/Cu solder joints. J. Electron. Mater. **37**, 1721–1726 (2008)
103. Q.L. Yang, J.K. Shang, Interfacial segregation of Bi during current stressing of Sn–Bi/Cu solder interconnect. J. Electron. Mater. **34**, 1363–1367 (2005)
104. F. Wang, L. Liu, D. Li, M. Wu, Electromigration behaviors in Sn–58Bi solder joints under different current densities and temperatures. J. Mater. Sci. Mater. Electron. **29**, 21157–21169 (2018)
105. D.L. Ma, P. Wu, Effects of coupled stressing and solid-state aging on the mechanical properties of Sn–58Bi–0.7Zn solder joint. J. Mater. Sci. Mater. Electron. **26**(8), 6285–6292 (2015)
106. H. He, G. Xu, F. Guo, Effect of small amount of rare earth addition on electromigration in eutectic SnBi solder reaction couple. J. Mater. Sci. **44**, 2089–2096 (2009)
107. T.W. Hu, Y. Li, Y.C. Chan, F.S. Wu, Effect of nano $Al_2O_3$ particles doping on electromigration and mechanical properties of Sn–58Bi solder joints. Microelectron. Reliab. **55**, 1226–1233 (2015)
108. L. Yang, J. Ge, Y. Zhang, J. Dai, Y. Jing, Electromigration reliability for $Al_2O_3$-reinforced Cu/Sn–58Bi/Cu composite solder joints. J. Mater. Sci. Mater. Electron. **28**, 3004–3012 (2017)
109. S. Ismathullakhan, H.Y. Lau, Y.C. Chan, Enhanced electromigration reliability via Ag nanoparticles modified eutectic Sn–58Bi solder joint. Microsyst. Technol. **19**, 1069–1080 (2013)
110. D.L. Ma, P. Wu, Effects of coupled stressing and solid-state aging on the mechanical properties of graphene nanosheets reinforced Sn–58Bi–0.7Zn solder joint. Mater. Sci. Eng. A **651**, 499–506 (2016)
111. G. Xu, F. Guo, X. Wang, Z. Xia, Y. Lei, Y. Shi, X. Li, Retarding the electromigration effects to the eutectic SnBi solder joints by micro-sized Ni-particles reinforcement approach. J. Alloy Compd **509**, 878–884 (2011)
112. X. Zhao, M. Saka, M. Muraoka, M. Yamashita, H. Hokazono, Electromigration behaviors and effects of addition elements on the formation of a Bi-rich layer in Sn58Bi-based solders. J. Electron. Mater. **43**, 4179–4185 (2014)
113. F. Wang, L. Zhou, Z. Zhang, J. Wang, X. Wang, M. Wu, Effect of Sn–Ag–Cu on the improvement of electromigration behavior in Sn–58Bi solder joint. J. Electron. Mater. **46**, 6204–6213 (2017)